UNCLASSIFIED

NAVAL PROVING GROUND

DAHLGREN, VIRGINIA

REPORT NO. 6-46

ANALYTICAL SUMMARY - PART I
THE PHYSICAL PROPERTIES OF STS UNDER TRIAXIAL STRESS

1 June 1946

BL

NPG Report # 6-7

S13-1(2)/L5-2(BXO 98155)

(b) If all references to "STS or Class B Armor", were replaced in the report by references to "Alloy Steel of 115000 (lb)/(in)^2 tensile strength", and if the references to individual Armor plates and classified reports were deleted, the report could be declassified for publication without further revision.

C. T. JOY

W. K. Mendenhall, Jr.
By direction.

Copy to: ~~Relf (7)(direct)~~
~~Adlf (4)(direct)~~

XL-2 AVH AVH:mas

XL

XA

XO BuOrd (Orig. + 2)

Report prepared by A.V. Hershey

Report reviewed by R. H. Lyddane
W. K. Mendenhall, Jr.

X File

UNCLASSIFIED

NAVAL PROVING GROUND
DAHLGREN, VIRGINIA

Rear Admiral C. T. Joy, USN
Commanding Officer

Captain W. K. Mendenhall, USN
Ordnance Officer

NPG Report No. 6-46

UNANNOUNCED

ANALYTICAL SUMMARY - PART I
The Physical Properties of STS Under Triaxial Stress.

Unclassified
(DATE) 8/31/76 B. Brayles (RANK) NavOrdLtr 0652/1178:PAH 5511 10/31/73

A. V. HERSHEY
Lt. Comdr., USNR

1 June 1946

NPG Report No. 6-46.

ANALYTICAL SUMMARY - PART I
The Physical Properties of STS Under
Triaxial Stress.

1. For some years the Naval Proving Ground has been assiduously engaged in the study of the penetration of armor by projectiles. Pursuance of this work to conclusive results must be predicated upon well substantiated theories defining the performances of the materials involved under the various possible conditions.

2. Particularly necessary in the more immediately practical field of armor study and evaluation is the need for dependable plate penetration charts or tables. In 1943 Lieut. Comdr. A. V. Hershey, USNR was assigned the task of preparing such charts. In prosecution of the assigned task he conducted an exhaustive study, employed for the first time new methods of attack and developed new theories concerning the phenomena incident to the penetration of plates by projectiles.

3. During the latter years of World War II, Lieut. Comdr. Hershey prepared a series of nine reports which are being published by the Naval Proving Ground under titles as follows:

(1) ANALYTICAL SUMMARY. PART I. THE PHYSICAL PROPERTIES OF STS UNDER TRIAXIAL STRESS.

Object: To summarize the available data on the physical properties of Class B Armor and STS under triaxial stress.

(2) ANALYTICAL SUMMARY. PART II. ELASTIC AND PLASTIC UNDULATIONS IN ARMOR PLATE.

Object: To analyse the propagation of undulations in armor plate; to summarize previous analytical work and to add new analytical work where required in order to complete the theory for ballistic applications.

(3) ANALYTICAL SUMMARY. PART III. PLASTIC FLOW IN ARMOR PLATE.

Object: To analyse the plastic flow in armor plate adjacent to the point of impact by a projectile.

(4) ANALYTICAL SUMMARY. PART IV. THE THEORY OF ARMOR PENETRATION.

Object: To summarize the theory of armor penetration in its present state of development, and to develop theoretical functions which can be used as a guide in the interpretation of ballistic data.

(5) BALLISTIC SUMMARY. PART I. THE DEPENDENCE OF LIMIT VELOCITY ON PLATE THICKNESS AND OBLIQUITY AT LOW OBLIQUITY.

Object: To compare the results of ballistic test with the prediction of existing formulae, and with the results of theoretical analysis; to find the mathematical functions which best represent the fundamental relationship between limit velocity, plate thickness, and obliquity at low obliquity.

(6) BALLISTIC SUMMARY. PART II. THE SCALE EFFECT AND THE OGIVE EFFECT.

Object: To determine the effect of scale on ballistic performance, and to correlate the projectile nose shape with the results of ballistic test.

(7) BALLISTIC SUMMARY. PART III. THE WINDSHIELD EFFECT, AND THE OBLIQUITY EFFECT FOR COMMON PROJECTILES.

Object: To analyse the action of a windshield during impact, and to develop mathematical functions which best represent the ballistic performance of common projectiles.

(8) BALLISTIC SUMMARY. PART IV. THE CAP EFFECT, AND THE OBLIQUITY EFFECT FOR AP PROJECTILES.

Object: To determine the action of a cap during impact, and to develop mathematical functions which best represent the ballistic performance of AP projectiles.

(9) BALLISTIC SUMMARY PART V. THE CONSTRUCTION OF PLATE PENETRATION CHARTS OR TABLES.

Object: To summarize the results of analysis in the form of standard charts or tables.

4. The opinions and statements contained in these reports are the expressions of the author, and do not necessarily represent the official views of the Naval Proving Ground.

C. T. Joy

C. T. JOY
Rear Admiral, USN
Commanding Officer

P R E F A C E

AUTHORIZATION

The material in this report is supplementary to the construction of plate penetration charts. It was authorized in BuOrd Letter NP9/A9 (Re3) dated 9 January 1943.

OBJECT

To summarize the available data on the physical properties of Class B Armor and STS under triaxial stress.

SUMMARY

The general analysis of stress and strain is applied to the data on STS and other steels to find mathematical functions which best represent the isothermal stress-strain relationship for STS under triaxial stress. Functions are given to represent the variation of shear stress with normal pressure, temperature, and strain rate. The adiabatic stress-strain relationship for STS under shear stress is derived and is applied to the propagation of plane plastic waves in STS. An analysis is made of the reflection of elastic waves from a free surface. Curves are given to represent the relationships between stress moments and curvatures in a bent plate.

TABLE OF CONTENTS

LIST OF TABLES

LIST OF FIGURES

I INTRODUCTION

A knowledge of the physical properties of armor steel under the conditions of impact is required in the analysis of the mechanics of armor penetration. The deformation near the impact hole is triaxial and varies from compression to shear.

There are available enough data to establish the stress-strain relationship for armor steel in the three limiting cases of tension, compression and shear. The stress-strain relationship for intermediate cases is found by interpolation with the aid of general formulae which have been established by tests on other metals.

The stress in armor steel which is subject to pure tension or pure compression has been determined at small strains by standard engineering tests, and has been investigated at large strains by Bridgman,[13,14,16]

The stress in armor steel which is subject to pure shear is difficult to measure because it is not easy to obtain homogeneous shear strains. In the conventional torsion test the shear strain varies from zero on the axis of the test specimen to a maximum at the surface. The strain would be more nearly uniform in a thin walled hollow cylinder, which is stressed by internal pressure, but local imperfections in the steel have been found to produce premature rupture[8,26] of the cylinder wall. Large shear strains in armor steel have been obtained with thick walled cylinders by Bridgman[15].

Enough measurements have been made at various pressures, temperatures, and strain rates to establish approximately the effects of pressure, temperature, and strain rate on the stress-strain relationship.

The available data for STS have been collected, and are summarized in the present report by curves which best represent the stress-strain-rate of strain relationship for STS of 115000 $(lb)/(in)^2$ tensile strength at a temperature of 15°C. These stress-strain-rate of strain relationships have been used in the analysis of a few simple examples of plastic deformation, which are of importance in connection with terminal ballistics.

The state of strain in the medium may be described either in terms of the linear components of strain or in terms of the natural components of strain. The linear strains are used in the present report, since they have a geometrical significance not possessed by the natural strains, and the stress-strain relationships happen to be symmetric in form when expressed in terms of linear strains. Since the analysis involves the general behavior of media under a polyaxial stress system, vector and tensor notation have been used.

II GENERAL ANALYSIS OF STRESS AND STRAIN

Elastic Media

Strain[1] in an elastic medium deforms a sphere into an ellipsoid, and applies to the components of a line segment in the medium a linear homogeneous transformation. Each particle of the medium experiences a vector displacement Δr which varies from point to point in the medium. The difference $d\Delta r$, between the displacements Δr and $\Delta r + d\Delta r$, of two points which were initially separated by the line segment dr, is given by the equation

$$d\Delta r = dr \cdot \nabla \Delta r$$

The two points are separated after deformation by the line segment $dr + d\Delta r$. The tensor $\nabla \Delta r$ is the sum of an antisymmetric tensor $\frac{1}{2}(\nabla \Delta r - \nabla^* \Delta r)$ and a symmetric tensor $\frac{1}{2}(\nabla \Delta r + \nabla^* \Delta r)$. The antisymmetric part is a rotation without strain if the displacements are small, and the symmetric part is a strain without rotation. A strain tensor Φ exists which may be defined in terms of displacement by the equation

$$\Phi = \tfrac{1}{2}(\nabla \Delta r + \nabla^* \Delta r) \tag{1}$$

The volume of a space initially enclosed by a surface s in the medium is increased on deformation by an amount given by the equation

$$\int \Delta r \cdot ds = \int \nabla \cdot \Delta r \, d\tau \tag{2}$$

A surface element in a medium under stress is acted upon by a force in the direction of stress. The magnitude of the force is proportional to the area of the projection of the surface element on a plane perpendicular to the direction of stress, which is just the component in the direction of stress of the vector representing the surface element. The scalar components of a force on a surface element are therefore obtained from the scalar components of the vector representing the surface element by a linear homogeneous transformation. A stress tensor Ψ exists, such that the force f on a closed surface s in the medium is given in terms of the stress tensor Ψ by the equation

$$f = \int \Psi \cdot ds = \int \nabla \cdot \Psi \, d\tau \tag{3}$$

The torque applied to a volume element is equal to the rate of increase of angular momentum of the volume element. The torque applied by an antisymmetric stress tensor decreases with decrease in the size of the element at a rate proportional to the cube of the linear dimensions of

the element, whereas the moment of inertia decreases at a rate proportional to the fifth power of the linear dimensions. The torque for a finite angular acceleration vanishes therefore in the limit as the size of the element is decreased, and the stress tensor is symmetric.

The stress tensor may be expressed in terms of the three principal stresses X_1, X_2, X_3 and the orthogonal unitary vectors i,j,k, which are collinear with the principal axes of stress, by the equation

$$\Psi = X_1 ii + X_2 jj + X_3 kk \tag{4}$$

The stress exerts upon any surface element of unit area with the normal n a force $\Psi \cdot n$ which may be resolved into a normal component $nn \cdot \Psi \cdot n$ in the direction of n and a shear component $\Psi \cdot n - nn \cdot \Psi \cdot n$ along the surface element. The normal component has a maximum or minimum value whenever n coincides with one of the three principal axes i,j,k. The shear component is zero whenever n coincides with the axes i,j,k and is a maximum whenever n is equal to one of the three vectors $\frac{1}{\sqrt{2}}(i+j)$, $\frac{1}{\sqrt{2}}(j+k)$, $\frac{1}{\sqrt{2}}(k+i)$ which are midway between the principal axes. The stress exerts upon an octahedral plane, whose normal n is the vector $\frac{1}{\sqrt{3}}(i+j+k)$, a normal component $\frac{1}{3}(X_1 + X_2 + X_3)n$ and a shear component $\frac{1}{\sqrt{3}}(X_1 i + X_2 j + X_3 k) - \frac{1}{3}(X_1 + X_2 + X_3)n$. The stress therefore exerts upon each face of an elementary octahedron, with axes parallel to the principal axes of stress, a normal stress of magnitude $\frac{1}{3}(X_1 + X_2 + X_3)$ and a shear stress of magnitude

$$\frac{1}{3}\sqrt{(X_1 - X_2)^2 + (X_2 - X_3)^2 + (X_3 - X_1)^2}$$

In an isotropic elastic medium the principal axes of strain are collinear with the principal axes of stress and the principal components of strain e_1, e_2, e_3 are related to the principal components of stress X_1, X_2, X_3 by the generalized Hooke's law

$$\begin{aligned} e_1 &= +\frac{1}{E}X_1 - \frac{\sigma}{E}X_2 - \frac{\sigma}{E}X_3 \\ e_2 &= -\frac{\sigma}{E}X_1 + \frac{1}{E}X_2 - \frac{\sigma}{E}X_3 \\ e_3 &= -\frac{\sigma}{E}X_1 - \frac{\sigma}{E}X_2 + \frac{1}{E}X_3 \end{aligned} \tag{5}$$

in which E is Young's modulus and σ is Poisson's ratio. These equations

may be written in the alternative form

$$e_1 + e_2 + e_3 = \frac{1-2\sigma}{E}(X_1 + X_2 + X_3) \tag{6}$$

$$\begin{aligned} e_1 - e_2 &= \frac{1+\sigma}{E}(X_1 - X_2) \\ e_2 - e_3 &= \frac{1+\sigma}{E}(X_2 - X_3) \\ e_3 - e_1 &= \frac{1+\sigma}{E}(X_3 - X_1) \end{aligned} \tag{7}$$

The dilation $e_1 + e_2 + e_3$ is expressed in terms of the mean hydrostatic tension $\frac{1}{3}(X_1 + X_2 + X_3)$ by the equation

$$e_1 + e_2 + e_3 = \frac{3(1-2\sigma)}{E}\,\frac{1}{3}(X_1 + X_2 + X_3) \tag{8}$$

and the octahedral shear strain $\frac{1}{3}\sqrt{(e_1-e_2)^2 + (e_2-e_3)^2 + (e_3-e_1)^2}$ is given in terms of the octahedral shear stress

$$\frac{1}{3}\sqrt{(X_1-X_2)^2 + (X_2-X_3)^2 + (X_3-X_1)^2}$$

by the equation

$$\tfrac{1}{3}\sqrt{(e_1-e_2)^2+(e_2-e_3)^2+(e_3-e_1)^2} = \frac{1+\sigma}{E}\,\tfrac{1}{3}\sqrt{(X_1-X_2)^2+(X_2-X_3)^2+(X_3-X_1)^2} \tag{9}$$

The energy w per unit volume of the medium is given by the equation

$$w = \frac{(1-2\sigma)}{6E}(X_1+X_2+X_3)^2 + \frac{(1+\sigma)}{6E}\{(X_1-X_2)^2+(X_2-X_3)^2+(X_3-X_1)^2\} \tag{10}$$

Solution of the equations of Hooke's law for X_1, X_2, X_3 in terms of e_1, e_2, e_3 leads to the system of equations

$$\begin{aligned} X_1 &= \frac{(1-\sigma)Ee_1}{(1+\sigma)(1-2\sigma)} + \frac{\sigma Ee_2}{(1+\sigma)(1-2\sigma)} + \frac{\sigma Ee_3}{(1+\sigma)(1-2\sigma)} \\ X_2 &= \frac{\sigma Ee_1}{(1+\sigma)(1-2\sigma)} + \frac{(1-\sigma)Ee_2}{(1+\sigma)(1-2\sigma)} + \frac{\sigma Ee_3}{(1+\sigma)(1-2\sigma)} \\ X_3 &= \frac{\sigma Ee_1}{(1+\sigma)(1-2\sigma)} + \frac{\sigma Ee_2}{(1+\sigma)(1-2\sigma)} + \frac{(1-\sigma)Ee_3}{(1+\sigma)(1-2\sigma)} \end{aligned} \tag{11}$$

The elastic modulus λ, the shear modulus μ, and the bulk modulus $\varkappa$ are defined in terms of Young's modulus E and Poisson's ratio σ by the equations

$$\lambda = \frac{\sigma E}{(1+\sigma)(1-2\sigma)} \qquad \mu = \frac{E}{2(1+\sigma)} \tag{12}$$

$$\varkappa = \lambda + \tfrac{2}{3}\mu = \frac{E}{3(1-2\sigma)} \tag{13}$$

In an isotropic elastic medium the stress tensor Ψ is related to the strain tensor Φ by the equation

$$\Psi = \lambda\nabla\cdot\Delta r I + 2\mu\Phi \tag{14}$$

in which I is the unitary tensor, and the force per unit volume $\nabla\cdot\Psi$ is given by the equation

$$\nabla\cdot\Psi = (\lambda+\mu)\nabla\nabla\cdot\Delta r + \mu\nabla\cdot\nabla\Delta r \tag{15}$$

Plastic Media

Strain in a plastic medium produces a displacement in the medium whose components are not always small. A line element dr is transformed into the line element $dr\cdot(I + \nabla\Delta r)$, and a sphere of unit radius is deformed into an ellipsoid whose equation is

$$r\cdot(I + \nabla\Delta r)^{-1}\cdot(I + \nabla^*\Delta r)^{-1}\cdot r = 1 \tag{16}$$

The principal radii $1+e_1$, $1+e_2$, $1+e_3$ and the principal axes i', j', k' of the ellipsoid define a linear strain tensor Π, which is expressed by the equation

$$\Pi = e_1 i'i' + e_2 j'j' + e_3 k'k' \tag{17}$$

The principal axes of stress are not always collinear with the principal axes of strain. The stress tensor Ψ, when referred to the axes i', j', k' of the ellipsoid has all of the components in the matrix

$$\begin{Vmatrix} X_{11} & X_{12} & X_{31} \\ X_{12} & X_{22} & X_{23} \\ X_{31} & X_{23} & X_{33} \end{Vmatrix}$$

The mean hydrostatic tension $\frac{1}{3}\Sigma X_m$ is given in terms of the components by the invariant equation

$$\tfrac{1}{3}\Sigma X_m = \tfrac{1}{3}(X_{11} + X_{22} + X_{33}) \tag{18}$$

and the octahedral shear stress $\frac{1}{3}\sqrt{\Sigma(X_m - X_n)^2}$ is given by the invariant equation

$$\tfrac{1}{3}\sqrt{\Sigma(X_m - X_n)^2} = \tfrac{1}{3}\sqrt{2}(X_{11}^2 + X_{22}^2 + X_{33}^2 - X_{11}X_{22} - X_{22}X_{33} - X_{33}X_{11} + 3X_{12}^2 + 3X_{23}^2 + 3X_{31}^2)^{\frac{1}{2}} \tag{19}$$

Plastic flow in a medium occurs with a particle velocity v which varies from point to point in the medium. The gradient ∇v of v may be resolved into a symmetric part and an antisymmetric part. The symmetric part Σ is the rate of strain, and is expressed by the equation

$$\Sigma = \tfrac{1}{2}(\nabla v + \nabla^* v) \tag{20}$$

The antisymmetric part Ω is the rate of rotation, and is expressed by the equation

$$\Omega = \tfrac{1}{2}(\nabla v - \nabla^* v) \tag{21}$$

The rate of strain Σ, when referred to the axes i', j', k', has all of the components in the matrix.

$$\begin{Vmatrix} \dot{\epsilon}_{11} & \dot{\epsilon}_{12} & \dot{\epsilon}_{31} \\ \dot{\epsilon}_{12} & \dot{\epsilon}_{22} & \dot{\epsilon}_{23} \\ \dot{\epsilon}_{31} & \dot{\epsilon}_{23} & \dot{\epsilon}_{33} \end{Vmatrix}$$

with principal components $\dot{\epsilon}_1$, $\dot{\epsilon}_2$, $\dot{\epsilon}_3$. A unit volume of the medium increases in volume at a rate $\nabla \cdot v$ which is expressed in terms of $\dot{\epsilon}_1$, $\dot{\epsilon}_2$, $\dot{\epsilon}_3$ by the equation

$$\nabla \cdot v = \dot{\epsilon}_1 + \dot{\epsilon}_2 + \dot{\epsilon}_3 \tag{22}$$

The components of rate of shear in the medium are the differences $\dot{\epsilon}_1 - \dot{\epsilon}_2$, $\dot{\epsilon}_2 - \dot{\epsilon}_3$, $\dot{\epsilon}_3 - \dot{\epsilon}_1$ between the components of rate of strain.

In an isotropic plastic medium, the principal axes of stress are collinear with the principal axes of rate of strain, but the components of stress are functions of the components of rate of strain, the linear strain and the previous history of the medium.

The state of stress[2] in a polyaxial stress system may be represented graphically by a point in a three dimensional cartesian space, whose coordinates are the principal components of stress. The state of strain may similarly be represented graphically by a point in a three dimensional cartesian space, whose coordinates are the principal components of strain. For a particular element of the medium there is a line in each space which traces out the stress or strain as a function of time, and corresponds, in parametric form, to the stress-strain curve for a uniaxial stress system.

The cartesian coordinates, X_1, X_2, X_3 of a point in stress space may be expressed in terms of a set of cylindrical polar coordinates, whose polar axis makes equal angles with the three principal axes of stress. The point in stress space lies on that octahedral plane which is situated at a distance $\frac{1}{\sqrt{3}}(X_1 + X_2 + X_3)$ from the origin as measured along the octahedral axis. The distance from the point to the octahedral axis is $\frac{1}{\sqrt{3}}\sqrt{(X_1-X_2)^2 + (X_2-X_3)^2 + (X_3-X_1)^2}$ as measured in the octahedral plane. The orientation of the point with respect to the octahedral axis may be represented graphically by a projection of the point on the octahedral plane, together with projections of the coordinate axes. Two stress-strain curves in stress space which differ only by the amount of hydrostatic tension have almost identical projections on the octahedral plane.

The cartesian coordinates e_1, e_2, e_3 of a point in strain space may similarly be expressed in terms of the cylindrical polar coordinates $\frac{1}{\sqrt{3}}(e_1+e_2+e_3)$ and $\frac{1}{\sqrt{3}}\sqrt{(e_1-e_2)^2+(e_2-e_3)^2+(e_3-e_1)^2}$ and the orientation of the point in strain space with respect to the octahedral axis may be represented by a projection on the octahedral plane. All points in strain space for a particular value of the hydrostatic tension lie on a curved surface which is normal to the octahedral axis, at the point where it intersects the axis.

The conditions that govern the plastic deformation in a polyaxial stress system are the equation of continuity

$$(1+e_1)(1+e_2)(1+e_3) = 1+\frac{1}{\kappa}\frac{1}{3}(I_1+I_2+I_3) \tag{23}$$

and the equations of flow,

$$\begin{aligned}
\dot{\epsilon}_1-\dot{\epsilon}_2 &= \frac{1+\sigma}{E}(\dot{I}_1-\dot{I}_2)+f_1\{(I_1-I_2),(I_2-I_3),(I_3-I_1)\}\{+2f_2(I_1-I_2)-f_2(I_2-I_3)-f_2(I_3-I_1)\}\\
\dot{\epsilon}_2-\dot{\epsilon}_3 &= \frac{1+\sigma}{E}(\dot{I}_2-\dot{I}_3)+f_1\{(I_1-I_2),(I_2-I_3),(I_3-I_1)\}\{-f_2(I_1-I_2)+2f_2(I_2-I_3)-f_2(I_3-I_1)\}\\
\dot{\epsilon}_2-\dot{\epsilon}_1 &= \frac{1+\sigma}{E}(\dot{I}_3-\dot{I}_1)+f_1\{(I_1-I_2),(I_2-I_3),(I_3-I_1)\}\{-f_2(I_1-I_2)-f_2(I_2-I_3)+2f_2(I_3-I_1)\}
\end{aligned} \tag{24}$$

in which the functions f_1 and f_2 determine the magnitude and distribution of rate of shear among the three components of rate of shear.

In the special case of a medium which obeys the Mohr[9] criterion, plastic deformation occurs only if one or more of the maximum shear stresses is equal to a critical yield stress and shear in the medium occurs only on that plane on which the shear stress is a maximum. The stress is represented in stress space by a hexagonal prism whose axis makes equal angles with the three principal axes of stress, and the projection on the octahedral plane is a hexagon. The projection is illustrated schematically in Figure (1) and functions for the equations of flow are given in Table I.

In the special case of a medium which obeys the vonMises[8] criterion, plastic deformation occurs only if the octahedral shear stress is equal to a critical yield stress, and the components of rate of shear are proportional to the components of shear stress. The stress is represented in stress space by a circular cylinder whose axis makes equal angles with the three principal axes of stress, and its projection on the octahedral plane is a circle. The projection is illustrated in Figure (1) and the functions in the equations of flow are given in Table I.

In the special case of a medium which obeys the Bailey[7] criterion, the functions f_1 and f_2 are power laws. The octahedral shear stress for a particular rate of strain is constant, but the components of rate of shear are only proportional to the components of shear stress in the case of pure tension, compression or shear. The projection on the octahedral plane is illustrated in Figure (1) and the functions are given in Table I.

The actual medium obeys the Bailey criterion in the neighborhood of the yield point but more complicated functions are required for stresses far above the yield point. The loci of points in stress space for unit octahedral shear strain are illustrated in Figure (2). The points connected by Curve I represent the stress required to deform the original material with the stress ratios held constant. The points labeled *A* represent the stress required to deform, by tension, compression, or torsion, a medium which has been prestrained in tension. The octahedral shear stress required for shear is much less than the octahedral shear stress required for tension or compression. The octahedral shear stress required for torsion is nearly the same for a prestrain in tension as it is for a prestrain in torsion. The conditions for plastic flow with the stress ratios held constant are therefore nearly valid also for deformations in which the stress ratios vary, or in which the principal axes of stress rotate. Curve I is symmetric about the octahedral axis, with three axes of symmetry, and a function of the sixth degree is required to represent it, such as the function in the last line of Table I.

If the pressure, temperature, and strain rate modify the stress by ratios which are independent of strain, then the parameters α, β, γ in Table I may be expressed as functions of the octahedral shear strain only, for a static deformation at standard pressure and temperature, and the parameter q, defined by the equation

$$q = \{\alpha((X_1-X_2)^2 + (X_2-X_3)^2 + (X_3-X_1)^2)^3 + \beta(X_1-X_2)^2(X_2-X_3)^2(X_3-X_1)^2\}^{\frac{1}{6}} \quad (25)$$

is then proportional to the ratio between the stress in an actual deformation and the stress in the static deformation. The parameters α, β may be so adjusted that q is equal to unity in a static deformation. It is also convenient to so define γ that the function $f_2(X_1-X_2)$ is equal to unity in a static deformation under pure tension. The parameter q may be represented as the product of three parameters, q_1, q_2, q_3 which are functions respectively of pressure, temperature, and strain rate. The function $f_1\{(X_1-X_2),(X_2-X_3),(X_3-X_1)\}$ is then a function of q_3 alone.

III THE DATA FOR STS AND OTHER STEELS

Elastic Properties

The data on the elastic constants for polycrystalline iron are summarized in the Metals Handbook[12]. Average values are reproduced in Table VI.

Plastic Properties

The Yield Stress

The behavior of armor steel near the yield point is probably the same as the behavior of the hollow steel cylinders in the tests made by Lode[4], by Taylor and Quinney[5], and by Davis[6], which were all found to have a nearly constant octahedral shear stress at the yield point. The octahedral shear stress for mild steel was found to become a function of the stress ratios, however, as the strain was increased above the yield point, with an octahedral shear stress for shear which was less than the octahedral shear stress for tension. Davis' data for mild steel are not in disagreement with the sixth power law for f_1 which has been adopted for armor in this report.

A more nearly complete investigation has been made of copper cylinders by Davis[7], who compared the test results with Bailey's formulae, and found good agreement with a fourth power law for f_2. Taylor and Quinney's results for mild steel are similar to the results for copper, and the same law for f_2 holds for both. A fourth power law has therefore been adopted also for armor steel.

Tension or Compression

In the case of pure tension or compression the principal axes of stress and strain remain collinear throughout. The stress is uniaxial and two components of strain are equal. The octahedral shear stress is given in terms of the single component of stress X_1 by the expression $\frac{1}{3}\sqrt{2}\,X_1$ and the hydrostatic tension is equal to $\frac{1}{3}X_1$. The octahedral shear strain is given in terms of the component e_1 along the axis of stress and the component $e_2 = e_3$ perpendicular to the axis of stress by the expression $\frac{1}{3}\sqrt{2}\,(e_1 - e_2)$. If e_1 and e_2 are the permanent strains that remain after release of stress, then the product $(1+e_1)(1+e_2)^2$ is equal to unity and the octahedral shear strain is given by the expression

$$\frac{1}{3}\sqrt{2}\left(1+e_1 - \frac{1}{\sqrt{1+e_1}}\right)$$

The linear strain Π has the components in the matrix

$$\begin{Vmatrix} e_1 & 0 & 0 \\ 0 & \frac{1}{\sqrt{1+e_1}} - 1 & 0 \\ 0 & 0 & \frac{1}{\sqrt{1+e_1}} - 1 \end{Vmatrix}$$

and the rate of strain Σ has the matrix

$$\begin{Vmatrix} \frac{\dot{e}_1}{1+e_1} & 0 & 0 \\ 0 & -\frac{1}{2}\frac{\dot{e}_1}{(1+e_1)} & 0 \\ 0 & 0 & -\frac{1}{2}\frac{\dot{e}_1}{(1+e_1)} \end{Vmatrix}$$

Values of the principal strains, the mean strain and the octahedral shear strain for a few values of the component of strain along the axis of stress are listed in Table II.

The available data on the stress-strain curves for Class B armor or STS are summarized in Figure (4). The data at small strains are summarized by Curve II, which represents the average of tensile tests at the Armor and Projectile Laboratory on a series of eight plates. The data for intermediate strains are summarized by Curve III, which represents the average of tensile tests at the California Institute of Technology[25] on three STS plates, and by Curve IV, which represents the average of compression tests at the Naval Gun Factory on four Class B armor plates*. The tensile test data for large strains were obtained by Bridgman[14] at Harvard University on these same four armor plates, while the compression test data at large strains were obtained on a different STS plate**.

The data in Figure (4) have all been corrected to a standard tensile strength of 115000 (lb)/(in)^2, and to zero hydrostatic tension. An asterisk is included in the figure to mark the point of maximum load in the tensile test. A single curve is adequate to represent the data for both tension and compression.

---

* Plates numbered DD419, 37813, 4A308A2 and 2A369A1.

**Plate No. 87207.

Torsion

In the case of pure torsion the stress is biaxial and the principal components of stress and strain normal to the surface of the specimen are both zero. Let i, j, k be unit vectors with k in the axial direction parallel to the axis of the specimen and i in the radial direction perpendicular to the axis. The displacement Δr of a point is given in terms of the conventional shear s by the equation

$$\Delta r = szj$$

in which z is the axial distance, before strain, of the point from a reference plane perpendicular to the axis. The conventional shear strain s at the surface of the specimen is defined in terms of the radius a of the specimen, the length l of the specimen and the twist ϕ by the equation

$$s = \frac{a\phi}{l}$$

The tensors $I + \nabla\Delta r$ and $(I + \nabla\Delta r)^{-1}$ have the matrices

$$\begin{Vmatrix} 1 & 0 & 0 \\ 0 & 1 & 0 \\ 0 & s & 1 \end{Vmatrix} \qquad \text{and} \qquad \begin{Vmatrix} 1 & 0 & 0 \\ 0 & 1 & 0 \\ 0 & -s & 1 \end{Vmatrix}$$

The tensor $(I+\nabla\Delta r)^{-1} \cdot (I + \nabla^*\Delta r)^{-1}$ has the matrix

$$\begin{Vmatrix} 1 & 0 & 0 \\ 0 & 1 & -s \\ 0 & -s & 1+s^2 \end{Vmatrix}$$

Its principal components are $1 + \frac{1}{2}s^2 \pm s\sqrt{1 + \frac{1}{4}s^2}$ and its principal axes j', k' make an angle θ with the axes j,k equal to $\frac{1}{2}\cot^{-1}(\frac{1}{2}s)$. The reciprocals of the principal components are the squares of the radii $1+e_2$, $1+e_3$ of the strain ellipsoid[28].

The principal radii, $1+e_2$, $1+e_3$ are given in terms of s by the equations

$$1+e_2 = + \tfrac{1}{2}s + \sqrt{1 + \tfrac{1}{4}s^2}$$

$$1+e_3 = - \tfrac{1}{2}s + \sqrt{1 + \tfrac{1}{4}s^2}$$

and the principal axes are given in terms of e_2 and e_3 by the equations

$$j' = + j\cos\theta + k\sin\theta = \frac{e_2 j - e_3 k}{\sqrt{e_2^2 + e_3^2}}$$

$$k' = - j\sin\theta + k\cos\theta = \frac{e_3 j + e_2 k}{\sqrt{e_2^2 + e_3^2}}$$

The linear strain tensor Π is equal to $e_2 j'j' + e_3 k'k'$ and has all of the terms in the matrix

$$\begin{Vmatrix} 0 & 0 & 0 \\ 0 & e_{22} & e_{23} \\ 0 & e_{32} & e_{33} \end{Vmatrix}$$

The components of the matrix are given in terms of s by the equations

$$e_{22} = - 1 + \sqrt{1 + \tfrac{1}{4}s^2} + \frac{\frac{1}{4}s^2}{\sqrt{1 + \frac{1}{4}s^2}}$$

$$e_{23} = \frac{\frac{1}{2}s}{\sqrt{1 + \frac{1}{4}s^2}} = e_{32}$$

$$e_{33} = - 1 + \sqrt{1 + \tfrac{1}{4}s^2} - \frac{\frac{1}{4}s^2}{\sqrt{1 + \frac{1}{4}s^2}}$$

The rate of strain tensor Σ has the components in the matrix

$$\begin{Vmatrix} 0 & 0 & 0 \\ 0 & 0 & \frac{1}{2}\dot{s} \\ 0 & \frac{1}{2}\dot{s} & 0 \end{Vmatrix}$$

A few of the functions for pure torsion are listed in Table III for a few values of s.

Stress-strain curves are reproduced in Figure (3) for annealed SAE 1020 Steel which were published by Zener and Hollomon[19]. Curve I is the experimental curve for stress against natural strain for the tension

test, Curve II is a plot of the octahedral shear stress against the octahedral shear strain in the tension test. Curve III is the stress strain curve in torsion to be expected for an isotropic medium with the same octahedral shear stress in shear as in tension, while Curve IV is the experimental curve for torsion. The octahedral shear stress for shear is lower than the octahedral shear stress for tension even at small strains where other tests indicate no discrepancy. The octahedral shear stress for torsion was 90% of the octahedral shear stress for tension at an octahedral shear strain of 0.2.

Similar results have been published by Davis[6] at the Westinghouse Research Laboratory for 0.35% carbon steel. The octahedral shear stress for torsion in this case was 92% of the octahedral shear stress for tension at an octahedral shear strain of 0.2.

Among the tests made by Davis[6] was a combined tension and torsion test with the ratio of elongation to twist held constant. The angle between the principal axis of strain and the axis of the specimen increased during the test from 30° to 33° at the surface of the specimen, while the angle between the principal axis of rate of strain and the axis of the specimen decreased from 29° to 26°. Since the ratio of twist to elongation was nearly constant, the ratio of shear stress to longitudinal stress should also be constant at the surface of the specimen, and should vary in direct proportion to the distance from the axis of the specimen. The ratio between torque and load would then be equal to the product of $\frac{1}{3}a$ and the ratio at the surface between shear stress and longitudinal stress. The principal axes of stress, calculated from the ratio of torque to load, followed accurately the principal axes of rate of strain.

Bridgman[16] at Harvard University has investigated the effect of prestrain in tension on the stress in tension, torsion, and compression. At an octahedral shear strain of 1.0, the octahedral shear stress required for torsion was 85% of the octahedral shear stress for tension, and the octahedral shear stress for compression was only 81% of the octahedral shear stress for tension.

Radial Expansion

In the case of pure radial expansion the principal axes of stress and strain remain collinear throughout and one component of strain is zero. The octahedral shear strain is given in terms of the two other components of strain by the expression $\frac{1}{3}\sqrt{2}\sqrt{e_1^2 - e_1 e_2 + e_2^2}$. If e_1 and e_2 are permanent strains that remain after release of stress,

then the product $(1+e_1)(1+e_2)$ is equal to unity, and the octahedral shear strain is given by the function tabulated in Table IV. The linear strain tensor Π has the matrix

$$\begin{Vmatrix} e_1 & 0 & 0 \\ 0 & \frac{1}{1+e_1} - 1 & 0 \\ 0 & 0 & 0 \end{Vmatrix}$$

and the rate of strain tensor Σ has the matrix

$$\begin{Vmatrix} \frac{\dot{e}_1}{1+e_1} & 0 & 0 \\ 0 & -\frac{\dot{e}_1}{1+e_1} & 0 \\ 0 & 0 & 0 \end{Vmatrix}$$

Bridgman[16] at Harvard University has investigated the collapse of hollow cylinders under the application of external pressure. He found that the external pressure is accurately a linear function of the logarithm of the ratio between the inner radius and the outer radius of the cylinder, and that the elongation of the cylinder is negligible. Let the radii of the cylinder before compression be a and b, with $a \ll b$, and let the radii after compression be a' and b'. A point which was at a radius r before compression is displaced by the compression to a radius r'. The volume displaced is given in terms of the radii by the equations

$$\pi(a'^2 - a^2) = \pi(b'^2 - b^2) = \pi(r'^2 - r^2)$$

The components of strain are given by the equations

$$1 + e_1 = \sqrt{1 + \frac{a^2 - a'^2}{r'^2}}$$

$$1 + e_2 = \frac{1}{1 + e_1}$$

$$e_3 = 0$$

The components of strain and the octahedral shear strain are therefore

functions of a parameter u, which is defined by the equation

$$u = \frac{r'}{\sqrt{a^2 - a'^2}}$$

Since the component of strain e_3 is zero, the components of stress must satisfy the relationships

$$X_1 - X_3 = X_3 - X_2 \qquad\qquad X_1 - X_2 = 2(X_1 - X_3)$$

$$\tfrac{1}{3}\sqrt{(X_1-X_2)^2 + (X_2-X_3)^2 + (X_3-X_1)^2} = \sqrt{\tfrac{2}{3}}(X_1 - X_3)$$

The components of stress X_1, X_2 are functions of r', and the equation of equilibrium is

$$\frac{\partial X_1}{\partial r'} + \frac{(X_1 - X_2)}{r'} = 0$$

If the stress difference (X_1-X_2) is expressed in terms of the octahedral shear stress, and if the octahedral shear stress is a function of the strain, then the equation may be solved by quadrature. The values of X_1 at the inner and outer walls of the cylinder are equal to the internal and external pressures on the walls. The internal pressure is zero but the external pressure p is given by the equation

$$p = +\sqrt{6}\int_{\sqrt{a^2 - a'^2}}^{\sqrt{b^2 - b'^2}} \frac{1}{u}\frac{1}{3}\sqrt{(X_1-X_2)^2 + (X_2-X_3)^2 + (X_3-X_1)^2}\, du$$

If the external pressure p is differentiated with respect to a', an expression is obtained which involves the octahedral shear stress at the surfaces of the cylinder only, and is not a function of the stress in the interior.

Bridgman's data may be summarized by the expressions given in Table V. The expressions for p have been differentiated with respect to a' and the results of differentiation have been used in the computation of the octahedral shear stress at the inner wall. The octahedral shear stress assumed for the outer wall was corrected for strain hardening. Included in Table V are two steels of nearly 115000 (lb)/(in)^2 and

60000 (lb)/(in)^2 tensile strength. A small correction may be applied to the stress for the difference between the actual and nominal values. The octahedral shear stress for a hollow cylinder with a tensile strength of 115000 (lb)/(in)^2 is compared with the octahedral shear stress for pure tension or compression in Figure (4), where it is represented by Curve V. The conventional shear stress in torsion, derived from a hollow cylinder with a tensile strength of 60000 (lb)/(in)^2, is compared with the conventional shear stress for the torsion test itself in Figure (3) where it is represented by Curve V.

The Isothermal Stress-Strain Relationship for STS

Consideration of all of the available information on the deformation of armor steel and similar materials leads to the stress-strain functions plotted in Figure (5) and listed in Table VII. The line in Figure (5) for shear is straight except at the lowest strains but the line for compression and tension is slightly curved at the upper end. Values of α, β, γ have been found from the curves for the case of a static isothermal deformation and are listed in Table VII.

Preferred Orientation in Crystalline Grains

A partial explanation for the difference between the octahedral shear stresses required for tension and shear may possibly exist in the crystallographic structure of severely deformed steel. The individual grains in an annealed polycrystalline medium have a random orientation, but as the plastic deformation progresses, the grains acquire a preferred orientation[9]. In the case of armor steel with less than 5% alloy content, the grains have a body-centered cubic lattice[11] at temperatures less than 500°C. The direction of slip in a body-centered cubic lattice is the 111 axis or body diagonal, and the plane of slip may be any one or a combination of several planes which contain the 111 axis. The principal planes of slip are the 110 and 112 planes. In the case of pure tension the grains take up a preferred orientation with a 110 axis or face diagonal in the direction of stress. In the case of pure compression the predominant orientation has a 111 axis or body diagonal in the direction of stress, although a few grains may also have a 100 axis or cube edge in the direction of stress. In the case of pure shear the predominant orientation has a 100 axis, or cube edge in the direction of compression, with a 110 axis or face diagonal in the direction of tension.

The preferred orientations are summarized in Table X. Included in the table are the principal components of strain along the axes of stress, produced by unit slip in the crystal along the axis of slip, and the maximum resolved shear stress on any plane of slip in the crystal for

unit stress applied to the medium. The octahedral shear stress in the medium for unit resolved shear stress on the axis of slip is equal to 1 in the case of pure tension. $\frac{2}{3}$ or 1 in the case of pure compression, and $\frac{1}{2}\sqrt{3}$ in the case of pure shear. The octahedral shear stress for shear in the crystal is therefore less than the octahedral shear stress for either tension or compression.

The medium is of course by no means a perfect crystal after severe cold work and quantitative agreement between the experimental results and predictions based on crystal plasticity are not to be expected, either because of differences in the rate of work hardening in the crystal or because of constraints applied to each crystal grain by adjacent grains.

The Variation of Shear Stress With Normal Pressure

Two shear stresses, which differ only in sign should both cause shear strain in an isotropic medium at the same magnitude of stress. The shear stress in the tensile test differs only in sign from the shear stress in the compression test, but the mean hydrostatic tensions also differ in sign. It is well known[3] that metals yield in the compression test at a greater stress than they yield in the tensile test. The difference in yield stress is illustrated for armor steel by the tests which were made in 1941 at the Naval Gun Factory on Class B armor of 115000 (lb)/(in)^2 tensile strength. The stress at maximum load in the tensile test was 129000 (lb)/(in)^2, but at the same octahedral shear strain in compression the stress was 135000 (lb)/(in)^2 which represents a 5% increase in shear stress per 100000 (lb)/(in)^2 increase in normal pressure. None of the difference in stress was the result of intrinsic anisotropy, since specimens were cut from the armor in the three axes normal to the plate, parallel to the direction of rolling, and transverse to the direction of rolling, and the only evidence of anisotropy occurred in the ductility. Bridgman[13, 14, 15] has shown directly that the application of hydrostatic pressure in the tensile test raises the shear stress by a ratio which is nearly independent of strain. The average increase in tensile strength was 12% in a pressure range from 100000 (lb)/(in)^2 to 250000 (lb)/(in)^2. The average increase in tensile strength per 100000 (lb)/(in)^2 increase in pressure is of the order of 6±2%.

The Variation of Stress with Temperature

The effect of temperature upon the physical properties of STS has been investigated by the group at the Naval Research Laboratory[18] where the Brinell hardness was measured for temperatures in the range from -183°C to +165°C. The values for Brinell hardness have been converted[20] into values for tensile strength, have been divided throughout

by the tensile strength for 15°C, and the ratios have been plotted in Figure (7). The data indicate that the tensile strength decreases 7.5% per 100°C rise in temperature at 15°C.

The effects of temperature and rate of strain on the tensile strength of copper, aluminum, iron and mild steel have been investigated by Manjoine and Nadai[28] at the Westinghouse Research Laboratory for temperatures in the range from 20°C to 1200°C and for rates of strain in the range from $10^{-6}(\text{sec})^{-1}$ to $1000\ (\text{sec})^{-1}$. Curves are included in Figure (7) to illustrate approximately the variation with temperature for mild steel.

The effect of temperature upon the tensile strength for temperatures in the range from -190°C to +20°C and for strain rates in the range from $10^{-4}(\text{sec})^{-1}$ to $0.01(\text{sec})^{-1}$ has been found by the group at Watertown Arsenal[20] to be accurately representable by an equation of the form

$$\log X^* = A + \frac{1}{n}\left(\log\dot{\epsilon} + \frac{Q}{RT}\right)$$

in which X^* is the tensile strength, $\dot{\epsilon}$ the strain rate, T the absolute temperature, R the gas constant, and A, n and Q are constants. The corresponding functions $q_2(T)$ and $q_3(\dot{\epsilon})$ have the form

$$q_2(T) = A' e^{\frac{\dot{\epsilon}}{nkT}} \qquad q_3(\dot{\epsilon}) = A''\dot{\epsilon}^{\frac{1}{n}}$$

in which A' and A'' are constants. The Watertown Arsenal data correspond to a decrease in tensile strength of 7% per 100°C rise in temperature at 15°C in the case of forged steel or tempered martensite, and a decrease of 6% per 100°C rise in temperature in the case of pearlite. The results for forged steel or tempered martensite are illustrated in Figure (7) by the line labelled Z.

The function $q_2(T)$ which has been chosen to represent the ratio between the tensile strength at temperature T and the tensile strength at 15°C is plotted in Figure (7) and tabulated in Table VIII.

The Variation of Stress with Rate of Strain

The variation of stress with rate of strain has not been systematically investigated over a wide range of strain rate on Class B armor or STS. Measurements have been reported by Seitz[21] at the

University of Pennsylvania and at the Carnegie Institute of Technology, in which the stress was found to be increased with increase in strain rate, by a ratio independent of strain. The stress was increased by 21% to 24% for an increase in strain rate from 1 $(sec)^{-1}$ to 1500 $(sec)^{-1}$. The specimens were small cylinders .171" diam × .375" length, and were tested in compression to 25% reduction in length. Points are plotted in Figure (8) to represent these data.

Measurements on STS have been made by the group at the California Institute of Technology[25], in which the tensile strength in an impact tensile test was compared with the conventional static tensile strength. The specimens were .3" diam × 8" gage length, and the impact velocity was in the range from 25 (ft)/(sec) to 200 (ft)/(sec). The ratio between dynamic tensile strength and static tensile strength has been calculated from the data, and the averages for three STS plates have been plotted against the average rate of strain in Figure (8). Included among the data from the California Institute of Technology were some results on two Class B armor plates which are consistent with the results on STS but more widely scattered. The von Karman[18] critical impact velocity for Class B armor or STS was found to be 200 (ft)/(sec), and the data are all below the critical velocity. Included in the diagram are the average results for three mild steel plates investigated at the California Institute of Technology[25]. The von Karman[24] critical impact velocity for mild steel was found to be between 125 (ft)/(sec) and 150 (ft)/(sec), and the California Institute of Technology data on mild steel therefore straddle the critical velocity.

The only systematic investigation over the whole range of strain rate has been made by Manjoine and Nadai[23] at the Westinghouse Research Laboratory on copper, aluminum, iron and mild steel. The specimens were .2" diam × 1" gage length. A curve is plotted in Figure (8) to illustrate the Westinghouse Research Laboratory data on mild steel at 20°C, together with two of their data for pure iron. The curve has a characteristic minimum in approximately the range of strain rate which occurs in the conventional static tensile test, and the curve is not linear. The Westinghouse Research Laboratory data on mild steel were below the von Karman critical velocity.

Measurements have also been made on mild steel by the Massachusetts Institute of Technology[27] but the impact velocity was above the von Karman critical velocity and the data are all low. The data from the Massachusetts Institute of Technology are also included in Figure (8) for comparison.

Measurements by the group at Watertown Arsenal at strain rates less than 0.01 $(sec)^{-1}$ correspond to an increase in tensile strength of 0.9% per unit increase in $\log \dot{\epsilon}$ in the case of forged steel, and an increase of 0.8% in the case of pearlite. Their results for forged steel are illustrated in Figure (8) by the line labelled Z. A variation of stress with strain rate of the same magnitude has also been observed by Bridgman[12] with torsion tests on 1020 plain carbon steel at strain rates less than 1.0 $(sec)^{-1}$.

The group at the California Institute of Technology have found that the ratio between dynamic and static tensile strength is greatest for pure iron and decreases with increase in the hardness of the ferrous alloys. Their average results for iron, MS, HTS, Class B Armor and STS are compared with their results for a few SAE and NE steels in Figure (9).

The data reported by Seitz, by the California Institute of Technology, and by the Westinghouse Research Laboratory were all obtained with high speed impact machines, in which the energy of a spinning wheel is transferred through a tup to the specimen by a trigger device. The data from the Massachusetts Institute of Technology were obtained with a device in which the source of energy was an exploding powder charge. In all cases the oscillograms were obscured somewhat by vibrations in the specimen and stress gauge. The vibrations were damped, however, and the average stress at maximum load should be a fairly accurate representation of the dynamic tensile strength, even though the yield point was obscured by vibration. Similarly, the rate of strain in each tensile specimen was not constant, but the multiple reflection of plastic waves from both ends of the specimen together with damping effects probably reduced the fluctuations in rate of strain to such an extend that the instantaneous rate of strain at maximum load was not far different from the average rate of strain, as long as the impact velocity was less than the von Karman critical velocity.

Measurements have been made by the group at the California Institute of Technology[26], in which hollow tubes were loaded, at various rates, with internal fluid pressure, and the fluctuations in strain rate, which are associated with plastic waves, were thus eliminated. The apparatus was so designed that the axial component of stress was essentially zero. The stress system was therefore a uniaxial tension, with the principal axis of stress in the circumferential direction. The ratio between the dynamic tensile strength and the static tensile strength has been calculated from the data and the values for each of three STS plates have been plotted in Figure (8). The values of the ratio are scattered over a wide range, which extends from unity to the values for tensile tests. The specimens were cut from the plates with

the axes of the specimens parallel to the direction of rolling in the plates. The circumferential direction in the specimen was therefore a direction of little ductility, and the specimens usually ruptured at a circumferential strain much less than the strain for maximum load. Some specimens developed cracks and leaked after very little strain, and were probably not homogeneous in structure.

The function $q_3(\dot{\epsilon})$, which has been chosen to represent the ratio between dynamic and static tensile strength for Class B armor and STS, is given as a function of $\dot{\epsilon}$ in Figure (8) by the curve labelled STS.

At the strain rates of importance in ballistic applications, the function may be represented analytically by the limiting equation

$$\log q_3(\dot{\epsilon}) = (.01 \pm .02) + (.04 \pm .01)\log\dot{\epsilon} \qquad (26)$$

which is satisfied by q_3 at high rates of strain.

The function $q_3(\dot{\epsilon})$ has for its inverse, the function $f_1(q_3)$ which is tabulated for a few values of q_3 in Table IX. In the special case of a tensile test, the equations of flow reduce to the equation

$$\frac{3}{2}\dot{\epsilon} = f_1(q_3)3q_3^4$$

IV APPLICATIONS

The Adiabatic Stress-Strain Relationship for STS

Work is done on each element of volume in a medium during a plastic deformation. The rate of doing work is equal to the trace or spur of the tensor $\Psi\cdot\Sigma$. In the special case of a deformation with stationary axes of stress the work w on unit volume is given in terms of the components of strain e_1, e_2, e_3 by the equation

$$w = \int(1+e_1)(1+e_2)(1+e_3)\left(\frac{X_1 de_1}{1+e_1} + \frac{X_2 de_2}{1+e_2} + \frac{X_3 de_3}{1+e_3}\right) \qquad (27)$$

Approximately 13% of this energy in steel is stored in the form of internal potential energy[10], and the remainder is released in the form of heat. In an adiabatic deformation the temperature rises and the stress is less than the stress in an isothermal deformation.

The temperature rise in an adiabatic deformation is governed by the differential equation

$$\rho c_p dT = g q_2(T) dw_0$$

in which ρ is the density of the medium, c_p is the specific heat, T is the temperature, dw_0 is the work done on unit volume in an isothermal deformation, and g is the fraction of energy converted into heat. The integral of the differential equation is

$$w_0 = \frac{1}{g} \int_{T_0}^{T} \frac{\rho c_p}{q_2(T)} \, dT \qquad (28)$$

in which T_0 is the initial temperature.

The results of integration are tabulated in Table VIII, as a function of temperature, for Class B armor or STS. Specific heats for the integration were taken from the Metals Handbook[12]. A curve to represent the relationship between octahedral shear stress and octahedral shear strain in an adiabatic deformation with pure shear is plotted in Figure (6) together with the temperature. The stress in the adiabatic deformation is a maximum at an octahedral shear strain of 0.5.

The deformation in any object is isothermal if the deformation occurs so slowly that thermal equilibrium is maintained, and is adiabatic if the heat of deformation is liberated before it can be conducted away.

If the rate of strain were so adjusted that the rate of liberation of heat were constant, the temperature would rise adiabatically at the beginning of deformation, but would approach a steady state temperature as the deformation progressed. The transition from adiabatic deformation to isothermal deformation depends upon the dimensions of the object.

As an example, the temperature at the center of a standard .505" diam x 1" gage length tensile test bar would lag to one half of the adiabatic temperature rise in a time interval of the order of 10 sec. If the duration of the tensile test is much greater that 10 sec the deformation is nearly isothermal and if it is much less than 10 sec it is nearly adiabatic. The elongation at maximum load in the case of Class B armor or STS is 12%, and the transition rate of strain is therefore of the order of .01 $(sec)^{-1}$ in a tensile test on armor. The stress at 12% elongation in an adiabatic deformation is, however, only 2% less than the stress in an isothermal deformation at the same rate of strain.

The Propagation of Elastic Waves

The equation of motion[1] in an elastic medium is

$$\rho\ddot{\Delta r} = (\lambda+\mu)\nabla\nabla\cdot\Delta r + \mu\nabla\cdot\nabla\Delta r \tag{29}$$

in which ρ is the density of the medium, Δr is the displacement of an element of the medium and $\ddot{\Delta r}$ is the acceleration of the element.

The displacement Δr may be expressed as the sum of two vectors, the gradient of a scalar function whose curl is identically zero, and the curl of a vector function whose divergence is identically zero. The equation of motion splits into two separate wave equations which govern the two component vector functions. The irrotational displacement satisfies the equation*

$$\rho\ddot{\Delta r} = (\lambda+2\mu)\nabla\cdot\nabla\Delta r \qquad (\nabla\times\Delta r = 0)$$

and the rotational displacement satisfies the equation

$$\rho\ddot{\Delta r} = \mu\nabla\cdot\nabla\Delta r \qquad (\nabla\cdot\Delta r = 0)$$

The component deformations are propagated with different velocities.

In a plane longitudinal or irrotational wave there is a component of strain e_1 in the direction of propagation but the components e_2, e_3 parallel to the wave front are zero. The dilatation is therefore equal to e_1. The components of stress are given by the equations

$$X_1 = \frac{(1-\sigma)Ee_1}{(1+\sigma)(1-2\sigma)} \qquad X_2 = X_3 = \sigma X_1$$

and the velocity of propagation c_1 by the equation

$$c_1 = \sqrt{\frac{\lambda+2\mu}{\rho}} = \sqrt{\frac{X_1}{\rho e_1}} \tag{30}$$

---

* A vector whose curl is zero satisfies the equation

$$\nabla\times\nabla\times\Delta r = \nabla\nabla\cdot\Delta r - \nabla\cdot\nabla\Delta r = 0$$

In a plane transverse or rotational wave there is a simple shear s in the plane of the wave front but the displacement in the direction of propagation is zero. The principal axes of strain are at 45° to the direction of propagation and the principal components of strain are given by the equations

$$e_1 = + \tfrac{1}{2}s = - e_3 \qquad e_2 = 0$$

The principal components of stress are given by the equations

$$X_1 = + \mu s = - X_3 \qquad X_2 = 0$$

and the velocity of propagation c_2 by the equation

$$c_2 = \sqrt{\frac{\mu}{\rho}} = \sqrt{\frac{X_1}{\rho s}} \tag{31}$$

A plane longitudinal wave is transformed by reflection at a free boundary into a pair of waves. Let i, j, k be unit vectors with k normal to the free boundary, and let n_1' be the normal to the incident longitudinal wave, n_1'' be the normal to the reflected longitudinal wave and n_2'' be the normal to the reflected transverse wave. The incident normal n_1' makes an angle of incidence θ_1 with the boundary normal k. The reflected normal n_1'' makes an angle of reflection equal to the angle of incidence, but the reflected normal n_2'' makes a different angle of reflection θ_2 with the boundary normal. The normals and angles are illustrated in Figure (10). Since the waves must remain in phase at the boundary, the angles θ_1 and θ_2 are related to the velocities c_1 and c_2 by the law

$$\frac{\sin\theta_1}{\sin\theta_2} = \frac{c_1}{c_2}$$

The normals are expressed in terms of the unit vectors by the equations

$$n_1' = i\sin\theta_1 - k\cos\theta_1$$

$$n_1'' = i\sin\theta_1 + k\cos\theta_1$$

$$n_2'' = i\sin\theta_2 + k\cos\theta_2$$

Displacement in the transverse wave occurs in the direction of the unit vector $i\cos\theta_2 - k\sin\theta_2$. A strain e' in the incident longitudinal wave,

a strain e'' in the reflected longitudinal wave, and a shear s'' in the reflected transverse wave combine to give a displacement Δr whose gradient has the components in the matrix

$$\begin{Vmatrix} +(e'+e'')\sin^2\theta_1 + s''\sin\theta_2\cos\theta_2 & 0 & -(e'-e'')\sin\theta_1\cos\theta_1 - s''\sin^2\theta_2 \\ 0 & 0 & 0 \\ -(e'-e'')\sin\theta_1\cos\theta_1 + s''\cos^2\theta_2 & 0 & +(e'+e'')\cos^2\theta_1 - s''\sin\theta_2\cos\theta_2 \end{Vmatrix}$$

The principal component of strain normal to the plane of incidence is zero.

Since the force on the free boundary is zero, the principal axes of stress at the boundary are parallel to the surface, and the principal component of stress normal to the surface is zero. The principal axes of strain are therefore also normal to the surface, and the vectors i, k which were orthogonal before deformation are still orthogonal after deformation. The condition of orthogonality is given to the first order in the strains, by the equation

$$2(e'-e'')\sin\theta_1\cos\theta_1 = s''(\cos^2\theta_2 - \sin^2\theta_2) \tag{32}$$

and the principal components of strain are given by the equations

$$e_1 = (e'+e'')\sin^2\theta_1 + s''\sin\theta_2\cos\theta_2$$

$$e_2 = 0$$

$$e_3 = (e'+e'')\cos^2\theta_1 - s''\sin\theta_2\cos\theta_2$$

Solution of the equations of Hooke's law with e_2 and X_3 equal to zero leads to the relationship

$$\frac{e_1+e_3}{e_1-e_3} = 1-2\sigma = \frac{c_2^2}{c_1^2-c_2^2} = \frac{\sin^2\theta_2}{\sin^2\theta_1 - \sin^2\theta_2}$$

which may be reduced to the equation

$$(e'+e'')\sin^2\theta_1 = \frac{2s''\sin^2\theta_2\cos\theta_2}{\cos^2\theta_2 - \sin^2\theta_2} \tag{33}$$

The equations (32) and (33) may be solved simultaneously to find e'' and s'' in terms of e' for any θ_1.

The two velocities c_1 and c_2 for longitudinal and transverse waves in steel are 19400 (ft)/(sec) and 10400 (ft)/(sec). The components of strain in the waves reflected from a free surface have been computed for steel. They are listed in Table XI and plotted in Figure (11).

The Propagation of Plastic Waves

Plastic deformations are propagated by waves of variable velocity. In a plane longitudinal or irrotational wave there is a component of strain e_1 in the direction of propagation, but the components e_2, e_3 parallel to the wave front are zero. The dilatation is therefore equal to e_1, and the octahedral shear strain is equal to $\frac{1}{3}\sqrt{2}\, e_1$. In addition to the component of stress X_1 in the direction of propagation, there are two equal components of stress X_2, X_3 parallel to the wave front. The octahedral shear stress is therefore equal to $\frac{1}{3}\sqrt{2}\,(X_1-X_2)$, or to $\frac{1}{3}\sqrt{2}\,(X_1-X_3)$. Since the mean hydrostatic tension is a function of the dilatation, and the octahedral shear stress is a function of the octahedral shear strain, both may be expressed as functions of e_1, and may be solved simultaneously for the component X_1 of stress in terms of the component e_1 of strain. The equation of motion[22] is

$$\rho\ddot{\Delta x} = \frac{\partial X_1}{\partial x} = \frac{dX_1}{de_1}\,\frac{\partial^2 \Delta x}{\partial x^2}$$

in which x is the initial position along the direction of propagation of a point whose displacement is Δx and ρ is the initial density. A particular solution of the equation of motion may be found by the method of von Karman[24]. The strain e_1 is set equal to a function $\Psi(x/t)$, and the displacement Δx is then given by the equation

$$\Delta x = -\int_x^\infty \Psi\left(\frac{x}{t}\right)dx$$

The particle velocity $\dot{\Delta x}$ is given by the equation

$$\dot{\Delta x} = \int_x^\infty \frac{x}{t^2}\Psi'\left(\frac{x}{t}\right)dx = -\int_0^{e_1}\left(\frac{x}{t}\right)de_1 \qquad (34)$$

Substitution of the function for Δx into the equation of motion leads to the relationship

$$\frac{x}{t} = \sqrt{\frac{1}{\rho}\,\frac{dX_1}{de_1}} \qquad (35)$$

The plastic wave velocity decreases with increase in strain, but is not less than eight tenths of the elastic wave velocity.

The phase velocity x/t for STS is represented by Curve I in Figure (12) and the particle velocity $\dot{\Delta x}$ is represented by Curve II.

In a plane transverse or rotational wave, the medium is subject to a simple shear of amount s. The octahedral shear strain is almost, but not quite equal to $(1/\sqrt{6})s$. The correct relationship is given in Table III. Displacement in the medium is propagated by a shear stress X_{12}. The octahedral shear stress is equal to $\sqrt{\frac{2}{3}}\, X_{12}$. The shear stress X_{12} can be expressed as a function of s and the equation of motion is

$$\rho \ddot{\Delta y} = \frac{\partial X_{12}}{\partial x} = \frac{dX_{12}}{ds} \frac{\partial^2 \Delta y}{\partial x^2}$$

in which Δy is the displacement, parallel to the wave front. The equation is similar in form to the equation of motion for a longitudinal wave. The phase velocity is given therefore by the equation

$$\frac{x}{t} = \sqrt{\frac{1}{\rho} \frac{dX_{12}}{ds}} \tag{36}$$

The phase velocity decreases with increase in strain and becomes zero at that strain for which the adiabatic stress strain curve has zero slope.

The phase velocity x/t for STS is represented by Curve I in Figure (13), and the particle velocity $\dot{\Delta y}$ is represented by Curve II.

Von Karman's analysis gives the motion in a plastic wave which starts from the origin at zero time. The wave is maintained by a constant stress at the origin, and the particle velocity is constant at the origin. If the stress is suddenly withdrawn, an elastic unloading wave is transmitted which moves faster than any part of the plastic wave and overtakes the plastic wave. Interaction between the unloading wave and the plastic wave sets up secondary waves which gradually transform the kinetic energy in the medium into plastic energy. The propagation of the plastic deformation continues long enough to convert all of the kinetic energy into plastic energy. Details of the motion in the general case of a variable stress at the origin must be found by a more complicated analysis than von Karman's. If the velocity and displacement are both specified at every point in the medium at zero time, then the velocity and displacement are determined for all subsequent time by the equation of motion. The velocity and displacement may be found by numerical integration of the equation of motion.

The Flexure of a Plate

In the case of pure flexure, the central plane of a plate is bent into a curved surface. On the concave side of the middle surface the material of the plate is compressed, while on the convex side it is stretched. The middle surface remains nearly free of strain. Forces are applied to the edges of the plate, but not to the free surfaces, hence two of the principal axes of stress at a free surface lie in the surface, while the principal component X_3 of stress normal to the plate is zero. Two of the principal axes of strain at the surface therefore also lie in the surface. A line segment which was normal to the free surface before flexure, is still normal after flexure, and is also nearly normal to the middle surface.

The principal components of strain e_1 and e_2 are given by the equations

$$e_1 = \varkappa_1 z \qquad\qquad e_2 = \varkappa_2 z \tag{37}$$

in which $\varkappa_1$ and $\varkappa_2$ are the principal curvatures of the plate.

The flexure of the plate is maintained by two stress moments M_1 and M_2 which are defined by the equations

$$M_1 = -\int_{-\frac{1}{2}h}^{+\frac{1}{2}h} X_1 z\,dz \qquad\qquad M_2 = -\int_{-\frac{1}{2}h}^{+\frac{1}{2}h} X_2 z\,dz$$

in which z is the distance measured from the middle surface and h is the thickness of the plate. The stress moments M_1 and M_2 are expressed in terms of $\varkappa_1$ and $\varkappa_2$ by the equations

$$M_1 = -\frac{1}{\varkappa_1^2}\int_{-\frac{1}{2}h\varkappa_1}^{+\frac{1}{2}h\varkappa_1} X_1 e_1\,de_1 \qquad\qquad M_2 = -\frac{1}{\varkappa_2^2}\int_{-\frac{1}{2}h\varkappa_2}^{+\frac{1}{2}h\varkappa_2} X_2 e_2\,de_2 \tag{38}$$

Each of the components of stress X_1 and X_2 are functions of both of the components of strain e_1 and e_2. Each of the stress moments M_1 and M_2 are therefore also functions of both components of curvature $\varkappa_1$ and $\varkappa_2$. The relationship between the moments and the curvatures is best represented by a diagram, in which contours of equal $(1/h^2)M_1$ or $(1/h^2)M_2$ are plotted against $\frac{1}{2}h\varkappa_1$ and $\frac{1}{2}h\varkappa_2$. The contour plot for $(1/h^2)M_2$ may be obtained from the contour plot for $(1/h^2)M_1$ by an interchange of $\varkappa_1$ and $\varkappa_2$. A few contours for STS of 115000 (lb)/(in)^2 tensile strength are plotted in Figure (14), and the data for the contours are given in Table XII.

V TABLES OF FUNCTIONS

Table I

Flow Functions for Plastic Deformation

Theory	$f_1\{(X_1-X_2),(X_2-X_3),(X_3-X_1)\}$	$f_2(X_1-X_2)$
Mohr*	$\lim_{n\to\infty}\left\{\left(\frac{X_1-X_2}{X'}\right)^n + \left(\frac{X_2-X_3}{X'}\right)^n + \left(\frac{X_3-X_1}{X'}\right)^n\right\}$	$\lim_{n\to\infty}\left(\frac{X_1-X_2}{X'}\right)^n$
von Mises	$\lim_{n\to\infty}\left\{\frac{(X_1-X_2)^2 + (X_2-X_3)^2 + (X_3-X_1)^2}{2X'^2}\right\}^n$	X_1-X_2
Bailey	$A\{(X_1-X_2)^2 + (X_2-X_3)^2 + (X_3-X_1)^2\}^m$	$(X_1-X_2)^{m-2m}$
NPG**	$A\left\{\frac{\alpha((X_1-X_2)^2+(X_2-X_3)^2+(X_3-X_1)^2)^3 + \beta(X_1-X_2)^2(X_2-X_3)^2(X_3-X_1)^2}{q_1^6 q_2^6}\right\}^{\frac{m}{6}}$	$\pm\frac{\gamma(X_1-X_2)^4}{q_1^4 q_2^4}$

* X' = yield stress in the tensile test

** $f_2(X_1-X_2)$ is $+\gamma(X_1-X_2)^4$ if (X_1-X_2) is positive, $-\gamma(X_1-X_2)^4$ if (X_1-X_2) is negative.

Table II

The Components of Strain in Tension or Compression

e_1	$e_2 = e_3$	$\frac{1}{3}\Sigma e_m$	$\frac{1}{3}\sqrt{\Sigma(e_m - e_n)^2}$	$\pm\log(1+e_1)$ $\pm 2\log(1+e_2)$
-.9	+2.16	+1.140	-1.442	-2.30
-.8	+1.236	+ .557	- .960	-1.609
-.7	+ .825	+ .317	- .719	-1.204
-.5	+ .414	+ .109	- .451	- .693
-.3	+ .195	+ .030	- .233	- .357
-.2	+ .118	+ .012	- .150	- .223
-.1	+ .054	+ .003	- .072	- .105
0	.000	.000	.000	.000
+.1	- .046	+ .003	+ .069	+ .095
+.2	- .087	+ .009	+ .135	+ .182
+.5	- .184	+ .044	+ .322	+ .406
+1.0	- .293	+ .138	+ .609	+ .693
+1.5	- .367	+ .255	+ .880	+ .916
+2.0	- .423	+ .365	+1.142	+1.099
+3	- .500	+ .667	+1.650	+1.386
+5	- .592	+1.272	+2.636	+1.79
+10	- .698	+2.868	+5.043	+2.40

Table III

The Components of Strain in Pure Torsion

s	$1+e_2$	$1+e_3$	θ	$\frac{1}{3}\Sigma e_m$	$\frac{1}{3}\sqrt{\Sigma(e_m-e_n)^2}$	e_{22}	$e_{23}=e_{32}$	e_{33}	$+\log(1+e_2)$ $-\log(1+e_3)$
0	1.000	1.000	45°	.000	.000	.000	.000	.000	.000
.1	1.051	.951	43.6°	.001	.0408	.003	.0499	-.0015	.050
.2	1.105	.905	42.2°	.003	.0817	.015	.0995	-.005	.100
.5	1.281	.781	38.0°	.021	.205	.092	.242	-.029	.248
1.0	1.618	.618	31.7°	.079	.412	.342	.447	-.106	.481
1.5	2.000	.500	26.6°	.167	.623	.700	.600	-.200	.693
2	2.414	.414	22.5°	.276	.839	1.121	.707	-.293	.881
3	3.303	.303	16.8°	.535	1.281	2.05	.832	-.445	1.195
5	5.19	.192	10.9°	1.128	2.19	4.01	.928	-.764	1.646
10	10.10	.099	5.6°	2.733	4.52	9.00	.980	-.804	2.312

Table IV

The Components of Strain in Radial Expansion

e_1	e_2	$\frac{1}{8}\Sigma e_m$	$\frac{1}{8}\sqrt{\Sigma(e_m-e_n)^2}$	$+\log(1+e_1)$ $-\log(1+e_2)$
0	0	0	0	.000
.1	-.091	.003	.078	.095
.2	-.167	.011	.150	.182
.3	-.231	.023	.217	.262
.5	-.333	.056	.342	.406
1.0	-.500	.167	.624	.693
1.5	-.600	.300	.883	.916
2.0	-.667	.444	1.133	1.099
3	-.750	.750	1.620	1.386
5	-.833	1.389	2.575	1.79
10	-.909	3.030	4.94	2.40

Table V

The Collapse of Hollow Cylinders

Steel	Tensile Strength	External Pressure
A5	104000	$+ 92000 + 165000 \log(a/a')$
A6	114000	$+110000 + 191000 \log(a/a')$
A7	170000	$+255000 + 245000 \log(a/a')$
A8	--	$+135000 + 219000 \log(a/a')$
P	57000	$+ 58000 + 112000 \log(a/a')$

Table VI

Elastic Constants of Iron

E (lb)/(in)^2	$\varkappa$ (lb)/(in)^2	μ (lb)/(in)^2	σ (calc.)	λ (lb)/(in)^2	$\lambda + \mu$ (lb)/(in)^2	ρ (lb)/(ft)^3
$(29.5)(10^6)$	$(25.2)(10^6)$	$(11.4)(10^6)$	.30	$(17.7)(10^6)$	$(29.1)(10^6)$	490

UNCLASSIFIED

Table VII

Isothermal Stress-Strain Functions for Class B Armor and STS

115000 (lb)/(in)^2 = tensile strength 15°C = temperature $\frac{1}{3}(X_1 + X_2 + X_3) = 0$

$\frac{1}{3}\sqrt{\Sigma(e_m - e_n)^2}$	Tension-Compression $\frac{1}{3}\sqrt{\Sigma(X_m - X_n)^2}$ (lb)/(in)^2	Shear $\frac{1}{3}\sqrt{\Sigma(X_m - X_n)^2}$ (lb)/(in)^2	$10^5\alpha^{\frac{1}{6}}$ (in)^2/(lb)	$10^5\beta^{\frac{1}{6}}$ (in)^2/(lb)	$10^5\gamma^{\frac{1}{4}}$ (in)^2/(lb)
000	0	0			
0005	11000	11000	3.02		4.27
.001	21000	21000	1.57		2.22
.002	37000	37000	.91		1.28
.003	43000	43000	.78		1.10
.004	45000	45000	.74	.77	1.04
.005	46500	46000	.71	.84	1.01
.01	50000	49000	.66	.94	.94
.02	54000	52000	.62	.96	.98
.05	59000	56000	.57	.96	.80
.0825	62000	58000	.54	.945	.76
.10	63000	58500	.53	.94	.75
.20	68000	62000	.49	.92	.69
.50	77000	66000	.43	.90	.61
1.0	85000	69000	.39	.88	.55
2	97000	73000	.34	.86	.48
5	118000	78000	.28	.82	.40
10	140000	82000	.24	.79	.34

Table VIII

Ratio between the Stress in an Adiabatic Deformation and the Stress in an Isothermal Deformation

T °C	$q_2(T)$	$(10^{-6})\int \frac{\rho c_p}{q_2(T)} dT$ (ft)(lb)/(ft)^3
-200	1.57	-10.8
-150	1.25	- 9.5
-100	1.125	- 7.3
- 80	1.094	- 6.2
- 60	1.068	- 5.0
- 40	1.046	- 3.8
- 20	1.026	- 2.5
0	1.009	- 1.1
+ 15	1.000	0.00
+ 20	.995	+ .37
+ 40	.980	+ 1.9
+ 60	.967	+ 3.4
+ 80	.955	+ 5.0
+100	.942	+ 6.7
+150	.91	+11.0
+200	.88	+15.8

Table IX

Strain Rate Function for Class B Armor or STS

115000 (lb)/(in)^2 = tensile strength
15°C = temperature

q_s	$f_1(q_s)$ $(sec)^{-1}$
1.0	.0005
1.1	.3
1.2	8.0
1.3	60
1.4	300
1.5	1200

Table X

Properties of a Body-centered Cubic Crystal

Stress	Tension	Compression		Shear
		(1)	(2)	
Preferred Orientation				
Axis of Tension	110			110
Axis of Compression		111	100	100
Component of Strain, per Unit Slip on 111 Axis				
In Axis of Tension	$+\frac{2}{3}\sqrt{2}$			$+\frac{2}{3}\sqrt{2}$
In Axis of Compression		$-\frac{2}{9}\sqrt{2}$	$-\frac{4}{9}\sqrt{2}$	$-\frac{2}{3}\sqrt{2}$
Maximum Resolved Shear Stress on 111 Axis per Unit Applied Stress	$\frac{1}{3}\sqrt{2}$	$\frac{2}{9}\sqrt{2}$	$\frac{1}{3}\sqrt{2}$	$\frac{2}{3}\sqrt{2}$
Octahedral Shear Stress for Unit Applied Stress	$\frac{1}{3}\sqrt{2}$	$\frac{1}{3}\sqrt{2}$	$\frac{1}{3}\sqrt{2}$	$\sqrt{\frac{2}{3}}$

Table XI

Reflection of Elastic Waves at a Free Boundary in STS

θ_1	$\sin\theta_1$	$\sin\theta_2$	$\frac{e''}{e'}$	$\frac{s''}{e'}$	$\frac{e_1}{e'}$	$\frac{e_2}{e'}$	$\frac{1}{e'^2}\sqrt{\Sigma(e_m-e_n)^2}$
0°	.000	.000	-1.000	.000	.000	.000	.000
5°	.087	.047	- .991	.347	.016	-.007	.010
10°	.174	.093	- .963	.683	.064	-.027	.038
15°	.259	.139	- .918	.997	.143	-.060	.080
20°	.342	.183	- .858	1.280	.247	-.105	.148
25°	.423	.227	- .785	1.524	.375	-.159	.224
30°	.500	.268	- .702	1.721	.519	-.221	.310
35°	.574	.307	- .613	1.869	.674	-.287	.403
40°	.643	.345	- .521	1.965	.833	-.354	.498
45°	.707	.379	- .432	2.009	.989	-.421	.591
50°	.766	.411	- .349	1.005	1.132	-.482	.677
55°	.819	.439	- .279	1.955	1.255	-.534	.750
60°	.866	.464	- .226	1.865	1.348	-.573	.805
65°	.906	.486	- .197	1.737	1.397	-.594	.835
70°	.940	.504	- .203	1.570	1.387	-.590	.829
75°	.966	.518	- .257	1.355	1.293	-.550	.773
80°	.985	.528	- .380	1.066	1.080	-.459	.645
85°	.996	.534	- .608	.650	.682	-.290	.408
90°	1.000	.536	-1.000	.000	.000	.000	.000

Table XII

The Moment-Curvature Relationship for STS of 115000 (lb)/(in)^2 Tensile Strength

$\frac{1}{h^2} M_1$	$\kappa_2 = 0$		$\kappa_1 = \kappa_2$		$\kappa_1 = 0$		$\kappa_1 = -\kappa_2$		$M_2 = 0$	
	$\frac{1}{2}h\kappa_1$	$\frac{1}{2}h\kappa_2$	$\frac{1}{2}h\kappa_1$	$\frac{1}{2}h\kappa_2$	$\frac{1}{2}h\kappa_1$	$\frac{1}{2}h\kappa_2$	$\frac{1}{2}h\kappa_1$	$\frac{1}{2}h\kappa_2$	$\frac{1}{2}h\kappa_1$	$\frac{1}{2}h\kappa_2$
5000	.000943	.000	.000758	.000758	.000	.00322	.00142	-.00142	.00112	-.00035
10000	.00193	"	.00150	.00150	"	.010	.0033	-.0033	.00222	-.00072
15000	.00304	"	.00237	.00237	"	.054	.0206	-.0206	.0035	-.00121
20000	.00452	"	.0038	.0038					.0059	-.00233
22000	.00542	"	.0050	.0050					.0081	-.0034
24000	.00680	"	.0071	.0071					.0123	-.0055
26000	.0092	"	.0118	.0118					.0214	-.0102
28000	.0138	"	.023	.023					.0407	-.0201
30000	.024	"	.046	.046					.082	-.0427

VI LIST OF SYMBOLS

a, b	radii of cylindrical specimen before deformation.
a', b'	radii of cylindrical specimen after deformation.
A, A', A''	empirical constants
α, β, γ	parameters in the stress-strain-rate of strain relationship.
c_1	phase velocity for elastic longitudinal wave.
c_2	phase velocity for elastic transverse wave.
c_p	specific heat.
$e_{11}, e_{22}, e_{33}, e_{12}, e_{23}, e_{31}$	components of linear strain.
e_1, e_2, e_3	principal components of strain.
$1+e_1,\ 1+e_2,\ 1+e_3$	principal radii of a unit sphere after deformation into an ellipsoid
$\log(1+e_1),\ \log(1+e_2),\ \log(1+e_3)$	components of natural strain.
$\dot{e}_1,\ \dot{e}_2,\ \dot{e}_3$	time rates of change of e_1, e_2, e_3.
Σe_m	dilatation.
$\frac{1}{3}\sqrt{\Sigma(e_m-e_n)^2}$	octahedral shear strain.
e'	strain in incident longitudinal wave.
e''	strain in reflected longitudinal wave.
$\dot{\epsilon}$	strain rate (tension).
$\dot{\epsilon}_{11}, \dot{\epsilon}_{22}, \dot{\epsilon}_{33}, \dot{\epsilon}_{12}, \dot{\epsilon}_{23}, \dot{\epsilon}_{31}$	components of strain rate.
$\dot{\epsilon}_1,\ \dot{\epsilon}_2,\ \dot{\epsilon}_3$	principal components of strain rate.
$(\dot{\epsilon}_1-\dot{\epsilon}_2),\ (\dot{\epsilon}_2-\dot{\epsilon}_3),\ (\dot{\epsilon}_3-\dot{\epsilon}_1)$	principal components of rate of shear.
E	Young's modulus.

f	vector force.
$f_1\{(X_1-X_2),(X_2-X_3),(X_3-X_1)\}$	function in the flow equations which determines the magnitude of rate of strain.
$f_2(X_1-X_2), f_2(X_2-X_3), f_2(X_3-X_1)$	functions in the flow equations which determine the distribution of rate of shear.
g	fraction of plastic work converted into heat.
h	plate thickness.
i,j,k	orthogonal unitary vectors, i axis of specimen (tension or compression). i radial direction (torsion or radial expansion). k axis of specimen (torsion or radial expansion). k normal to free boundary (wave reflection and bent plate)
i,j,k	principal axes of stress (general analysis).
i',j',k'	principal axes of strain (general analysis).
I	unitary tensor.
ν	bulk modulus.
κ_1, κ_2	components of curvature, or reciprocals of the radii of curvature (bent plate).
λ	elastic modulus.
μ	shear modulus.
m,n	indices.
M_1, M_2	stress moments (bent plate).
n	unit vector normal to a surface element.

n_1	normal to incident longitudinal wave.
n_1''	normal to reflected longitudinal wave.
n_2''	normal to reflected transverse wave.
Ω	rate of rotation tensor.
p	pressure.
φ	angle of twist.
Φ	strain tensor (elastic deformation).
Π	strain tensor (plastic deformation).
Ψ	stress tensor (general analysis).
q	ratio between the stress in an actual deformation, and the stress in a static deformation at zero hydrostatic tension and at 15°C.
$q_1(p)$	ratio between shear stress at normal pressure p and shear stress at zero pressure.
$q_2(T)$	ratio between shear stress at actual temperature T and shear stress at 15°C.
$q_3(\dot{\epsilon})$	ratio between shear stress at strain rate $\dot{\epsilon}$ and shear stress in a static deformation.
Q	heat of activation per mol.
r	position vector of a point in the medium.
Δr	vector displacement of a point in the medium.
$\dot{\Delta r}$	vector velocity of a point in the medium.
$\ddot{\Delta r}$	vector acceleration of a point in the medium.
$\nabla \Delta r$	tensor gradient of the vector Δr.
$\nabla^* \Delta r$	conjugate of $\nabla \Delta r$.

$\nabla \cdot \Delta r$	divergence of Δr.
r	radial coordinate before deformation.
r'	radial coordinate after deformation.
R	gas constant per mol.
ρ	density.
s	vector surface (general analysis).
s	shear strain.
s''	shear strain in reflected transverse wave.
$\dot{s}$	rate of shear.
σ	Poisson's ratio.
Σ	rate of strain tensor.
t	time (sec).
T	absolute temperature (°K).
T_0	initial temperature (15°C).
τ	volume.
θ	angle between principal axis of strain and axis of specimen (torsion)
θ_1	angle of incidence and angle of reflection for longitudinal wave.
θ_2	angle of reflection for transverse wave.
u	variable of integration.
v	vector velocity of a point in the medium.
∇v	tensor gradient of the vector v.
$\nabla^* v$	conjugate of ∇v.

$\nabla \cdot v$	divergence of v.
w	plastic energy per unit volume.
w_0	plastic energy in an isothermal deformation.
x, y, z	cartesian coordinates.
$X_{11}, X_{22}, X_{33}, X_{12}, X_{23}, X_{31}$	components of stress.
X_1, X_2, X_3	principal components of stress.
$\frac{1}{3}\Sigma X_m$	mean hydrostatic tension.
$\frac{1}{3}\sqrt{\Sigma(X_m - X_n)^2}$	octahedral shear stress.
X'	yield stress.
X^*	tensile strength.

VII REFERENCES

1. C. E. Weatherburn, "Advanced Vector Analysis" (G. Bell and Sons, Ltd, 1937) Chapter VIII; A. E. H. Love, "A Treatise on the Mathematical Theory of Elasticity" (Cambridge University Press, 1927) Chapters, I, II and III.

2. M. Gensamer, "Strength of Metals under Combined Stresses" (American Society for Metals, 1941) Chapter II; Haigh, "The Strain Energy Functions and the Elastic Limit," Engineering 109, 158, (1920); H. M. Westergaard, "On the Resistance of Ductile Materials to Combined Stresses" J. Franklin Inst, (May, 1920).

3. A Nadai, "Plasticity" (McGraw Hill Book Co. Inc. 1931), Chapters 12 and 13; O. Mohr, "Abhandlungen aus dem gebiete der technischen Mechanik" (W. Ernst u. Sohn, Berlin, 1914) 2nd Ed. page 192; H. Hencky, "Zur Theorie plastischer Deformationen", Z. ang. Math. u. Mech. 4, 323 (1924); H. Hencky "Uber das Wesen der plastischen Verformung", Z.V.D.I. 69, 695 (1925); R. von Mises "Mechanik der festen Körper im plastisch-deformablen Zustand", Nachr. d. Gesellsch. d. Wissensch. zu. Göttingen, Math.-phys. Klasse, 1913.

4. W. Lode "Versuche uber den Einfluss den Mittleren Hauptspannung auf das Fliessen den Metalle Eisen, Kupfer und Nickel", Zeit. f. Physik, 36 913 (1926), Forschungsarbeiten, Heft 303 (V.D.I. Verlag, Berlin 1928).

5. G. I. Taylor and H. Quinney, "The Plastic Distortion of Metals", Phil. Trans. Roy. Soc. A230, 323 (1931).

6. E. A. Davis "Combined Tension-Torsion Tests on a 0.35% Carbon Steel" ASME Trans. 62 577 (1940).

7. E. A. Davis, "Increase of Stress with Permanent Strain and Stress-Strain Relations in the Plastic State for Copper under Combined Stresses", J. App. Mech. 10 A-187 (Dec. 1943); R. W. Bailey, "The Utilization of Creep Test Data in Engineering Design", J. Inst. Mech. Eng. 131, 131, (1935), and Engineering, 140, 595 and 647, (1935); H. J. Tapsell and A. E. Johnson, "Creep under combined Tension and Torsion", Engineering 150, 24 (1940).

8. E. A. Davis, " Yielding and Fracture of Medium Carbon Steel under Combined Stress", J. App. Mech. 12, A-13 (March 1945).

9. C. F. Elam "Distortion of Metal Crystals" (Oxford Clarendon Press, (1935), Chap. V; C. H. Mathewson, "Plastic Deformation of Iron" Metals Handbook (American Society for Metals, 1939) page 448.

10. C. F. Elam "Distortion of Metal Crystals" (Oxford Clarendon Press, 1935) Chap. XI; W. S. Farren and G. I. Taylor, Proc. Roy. Soc. A 107 422 (1925); G. I. Taylor and H. Quinney, "The Latent Energy Remaining in a Metal after Cold Working" Proc. Roy. Soc. 143A 307 (1934).

11. E. C. Bain and R. H. Aborn, "The Iron-Nickel-Chromium System", Metals Handbook (American Society for Metals, 1939) page 418.

12. R. L. Kenyon, "Physical and Mechanical Properties of Iron", Metals Handbook (American Society for Metals, Cleveland, 1939) page 424.

13. P. W. Bridgman, "Plastic Deformation of Steel Under High Pressure", NDRC Report No. A-95 (Sept. 1942).

14. P. W. Bridgman, "Third Progress Report on Plastic Deformation of Steel under High Pressure", NDRC Report No. A-218 (Sept. 1943); P. W. Bridgman, "Distortion of an Armor Plate Steel under Simple Compressive Stress to High Strains", NDRC Report No. A-235 (Dec. 1943).

15. P. W. Bridgman, "The Collapse of Hollow Cylinders under External Pressure", Watertown Arsenal Report No. 111/7-3 (Oct. 1943).

16. P. W. Bridgman, "First Report on Tension Tests under Pressure for the Watertown Arsenal", Watertown Arsenal Report No. 111/7 (March 1943); P. W. Bridgman, "The Effect of Prestraining in Tension on the Behavior of Steel under Tension, Torsion, and Compression", Watertown Arsenal Report No. 111/7-2 (July, 1943); P. W. Bridgman, "The Shape of the Neck and the Fracture of Tension Specimens", Watertown Arsenal Report No. 111/7-4 (Jan. 1944); P. W. Bridgman, "The Stress Distribution at the Neck of a Tension Specimen" Trans ASM, 32, 553 (1944).

17. P. W. Bridgman, "Second Report on Torsion Experiments", Watertown Arsenal Report No. 111/7-1 (March 1943).

18. G. D. Kinzer, "Tenth Partial Report on Light Armor", Naval Research Laboratory Report No. O-1892 (June, 1942).

19. C. Zener and J. H. Hollomon, "Plastic Flow and Rupture of Metals-First Partial Report", Watertown Arsenal Report No. 732/10 (Mar. 1943).

20. C. Zener and D. van Winkle, "High Speed Testing", Watertown Arsenal - Report No. 111.2/16 (June, 1943); J. H. Hollomon and C. Zener, "Plastic Flow and Rupture of Metals - Second Partial Report", Watertown Arsenal Report No. 732/10-1 (July, 1943).

21. O. C. Simpson, E. L. Fireman, and J. S. Koehler "High Speed Compression Testing of Copper Crusher Cylinders and Spheres", NDRC Report No. A-257 (March 1944), F. Seitz, "The Testing of Metals in Compression at High Rates of Strain", NDRC Report No. A-174 (April 1943).

22. J. S. Koehler and F. Seitz, "The Stress Waves Produced in a Plate by a Plane Pressure Pulse", NDRC Report No. A-245 (Feb. 1944).

23. M. Manjoine and A. Nadai, "High Speed Tension Tests at Elevated Temperatures - Part I", Proc. ASTM 40 822 (1940); A. Nadai and M. Manjoine, "High Speed Tension Tests at Elevated Temperatures - Parts II and III", Trans. ASME 63 A-77 (1941); M. Manjoine, "Influence of Rate of Strain and Temperature on Yield Stresses of Mild Steel", J. App. Mech. 11, A-211 (Dec. 1944).

24. Th. von Karman, "On the Propagation of Plastic Deformation in Solids", NDRC Report No. A-29 (Jan. 1942); P. E. Duwez, "Preliminary Experiments on the Propagation of Plastic Deformation", NDRC Report Nos A-33 (Feb. 1942) and A-244 (Revision) (Feb. 1944); M. P. White and L. Griffis, "The Permanent Strain in a Uniform Bar due to Longitudinal Impact", NDRC Report No. A-71 (July, 1942); P. E. Duwez, D. S. Wood, and D. S. Clark, "The Propagation of Plastic Strain in Tension", NDRC Report No. A-99 (Oct. 1942); Th. von Karman, H. F. Bohnenblust and D. H. Hyers, "The Propagation of Plastic Waves in Tension Specimens of Finite Length - Theory and Methods of Integration", NDRC Report No. A-103 (Oct. 1942); P. E. Duwez, D. S. Wood and D. S. Clark, "The Influence of Specimen Length on Strain Propagation in Tension", NDRC Report No. A-105 (Oct. 1942); P. E. Duwez, D. S. Wood, D. S. Clark, and J. V. Charyk, "The Effect of Stopped Impact and Reflection on the Propagation of Plastic Strain in Tension", NDRC Report No. A-108 (Nov. 1942); H. F. Bohnenblust, J. V. Charyk and D. H. Hyers, "Graphical Solutions for Problems of Strain Propagation in Tension", NDRC Report No. A-131 (Jan. 1943); P. E. Duwez, D. S. Wood, and D. S. Clark, "Factors Influencing the Propagation of Plastic Strain in Long Tension Specimens", NDRC Report No. A-159 (March 1943); P. E. Duwez, D. S. Clark and D. S. Wood, "Discussion of Energy Measurements in Tension Impact Tests at the California Institute of Technology", NDRC Report No. A-217 (Sept. 1943); D. S. Wood, P. E. Duwez, and D. S. Clark, "The Influence of Specimen Dimensions and Shape on the Results of Tensile Impact Tests", NDRC Report No. A-237, (Dec. 1943).

25. P. E. Duwez, D. S. Clark, and D. S. Wood, "The Influence of Impact Velocity on the Tensile Properties of Plain Carbon Steels and of a Cast Steel Armor Plate", NDRC Report No. A-154, (March 1943); P. E. Duwez, D. S. Wood, and D. S. Clark, "Dynamic Tests of the Tensile Properties of SAE 1020 Steels, Armco Iron and 17ST Aluminum Alloy", NDRC Report No. A-182, (May, 1943); P. E. Duwez, D. S. Wood, and D. S. Clark, "The Influence of Impact Velocity on the Tensile Properties of Class B Armor Plate, Heat-treated Alloy Steels, and Stainless Steel", NDRC Report No. A-195 (July, 1943); D. S. Clark, P. E. Duwez, and D. S. Wood, "The Influence of Velocity on the Tensile Properties of a Carbon Steel, Two National Emergency Steels, and a Manganese Steel", NDRC Report No. A-241 (Jan. 1944); D. S. Clark, P. E. Duwez, and D. S. Wood, "The Influence of Impact Velocity on the Tensile Properties of Three Types of Ship Plate: MS, HTS, STS", NDRC Report No. A-261 (March 1944).

26. P. E. Duwez, H. E. Martens, D. A. Elmer, and D. S. Clark, "The Influence of Pure Strain Rate on the Tensile Properties of Three Types of Ship Plate", NDRC Report No. M-459 (Feb. 1945).

27. W. P. Roop, and H. I. Carrigan, "Properties of Medium Steel at High Rates of Loading", David Taylor Model Basin Report No. 503 (June, 1943); A. V. deForest, A. R. Anderson, and R. Fanning, "Report on Impact Research", MIT Report to DTMB (May, 1941); A. V. deForest, C. W. MacGregor and P. R. Shepler "Impact Research on Medium Steel" MIT Report to DTMB (Sept. 1942).

28. The squares of the principal radii are derived by A. Nadai, "Plasticity" (McGraw Hill Book Co., 1931) page 296, by a different analysis.

29. The Hardness Conversion Table, Metals Handbook, (American Society for Metals, 1939) page 127, was used in the conversion of hardness units.

FIGURE (1)

PROJECTIONS ON THE OCTAHEDRAL PLANE

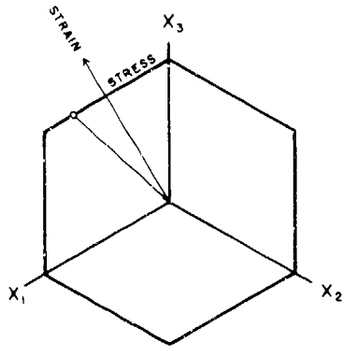

MOHR CRITERION

Strain occurs only in shear, stress may occupy any point on adjacent side of hexagon of stress

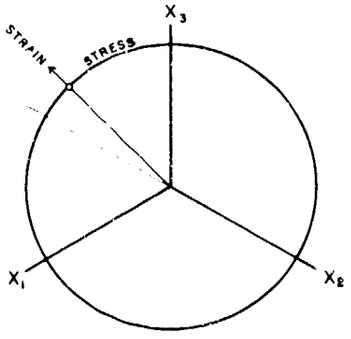

VON MISES CRITERION

Stress and strain are collinear

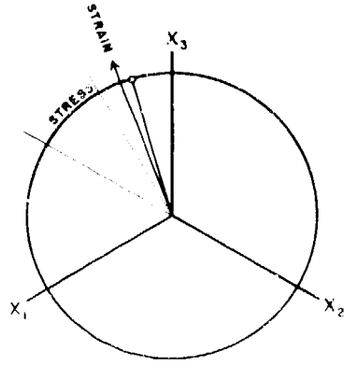

BAILEY CRITERION

Stress and strain are collinear for pure tension, compression or shear, but differ for intermediate stresses

NPG PHOTO NO. 3090 (APL)

FIGURE (2)

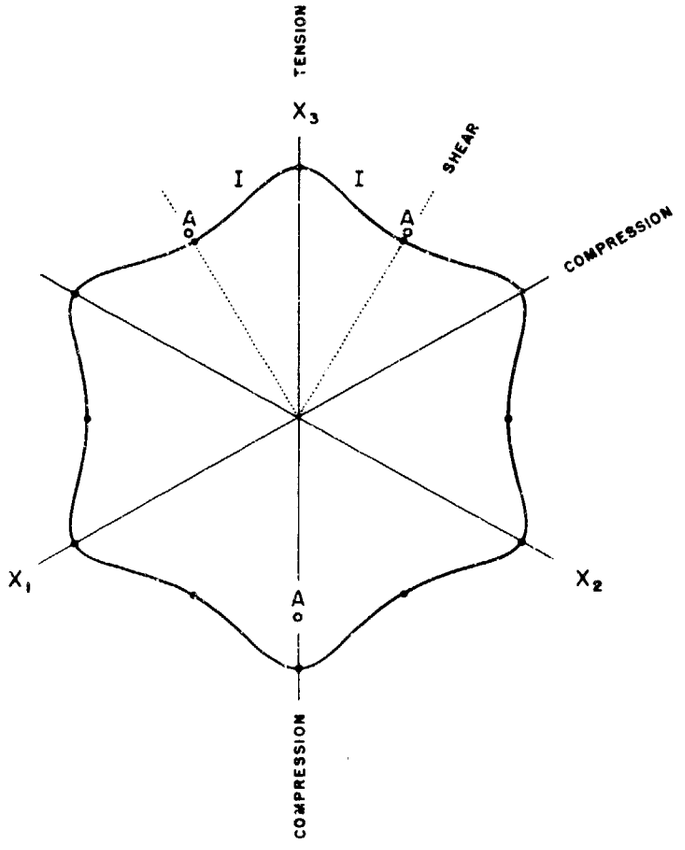

THE LOCI OF POINTS IN STRESS SPACE
FOR UNIT OCTAHEDRAL SHEAR STRAIN

NPG PHOTO NO. 3091 (APL)

FIGURE 13

COMPARISON OF STRESS IN TENSION AND TORSION

SAE 1020 Steel of 60000 $(lb)/(in)^2$ Tensile Strength

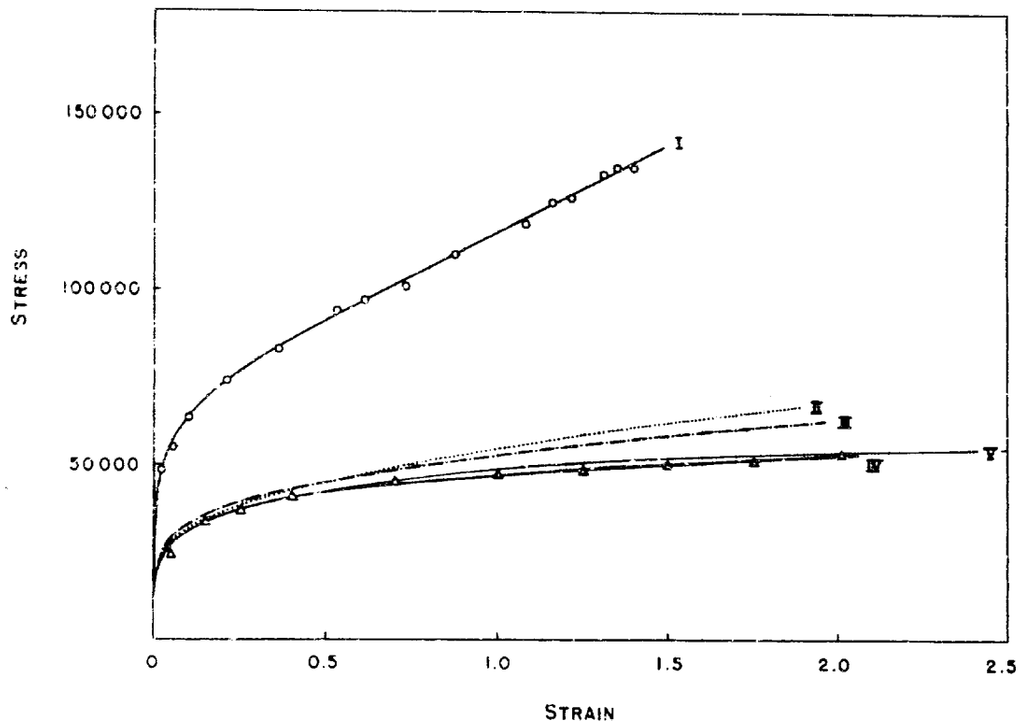

CURVE I	Watertown Arsenal Data			Tension Specimen	X_{33}	vs	$\log(1+e_3)$	
CURVE II	"	"	"	"	"	$\frac{1}{3}\sqrt{2}X_{33}$	vs	$\frac{1}{3}\sqrt{2}(1+e_3-\frac{1}{\sqrt{1+e_3}})$
CURVE III	"	"	"	"	"	X_{23}	vs	s
CURVE IV	"	"	"	Torsion Specimen		X_{23}	vs	s
CURVE V	Harvard University Data			Hollow Cylinder		X_{23}	vs	s

NRS PHOTO NO 3092 (APG)

FIGURE (4)

STRESS-STRAIN CURVES

The Isothermal Relationship between Octahedral Shear Stress and Octahedral Shear Strain for Zero Mean Hydrostatic Tension

Data for STS of 115000 $(lb)/(in)^2$ Tensile Strength

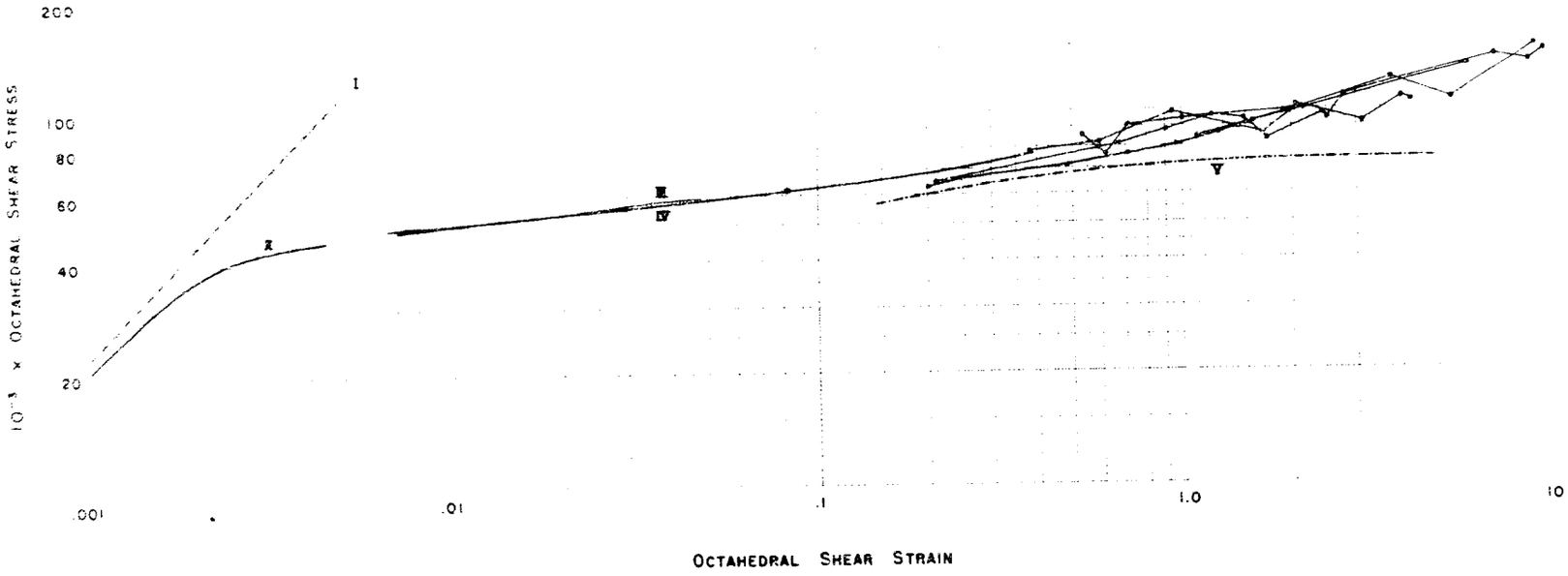

o—o Harvard University Data
Tensile Specimens at High Pressure

•—• Harvard University Data
Compression Specimens

CURVE I The Elastic Line

CURVE II Armor and Projectile Laboratory Data
Standard Tensile Test

CURVE III California Institute of Technology Data
Standard Tensile Test

CURVE IV Naval Gun Factory Data
Standard Compression Test

CURVE V Harvard University Data
Hollow Cylinders under External Pressure

PHOTO NO. 3093 (APL)

STRESS-STRAIN CURVES

FIGURE (5)

The Isothermal Relationship between Octahedral Shear Stress and Octahedral Shear Strain for Zero Mean Hydrostatic Tension

Average Curves for STS of 115000 (lb)/(in)^2 Tensile Strength

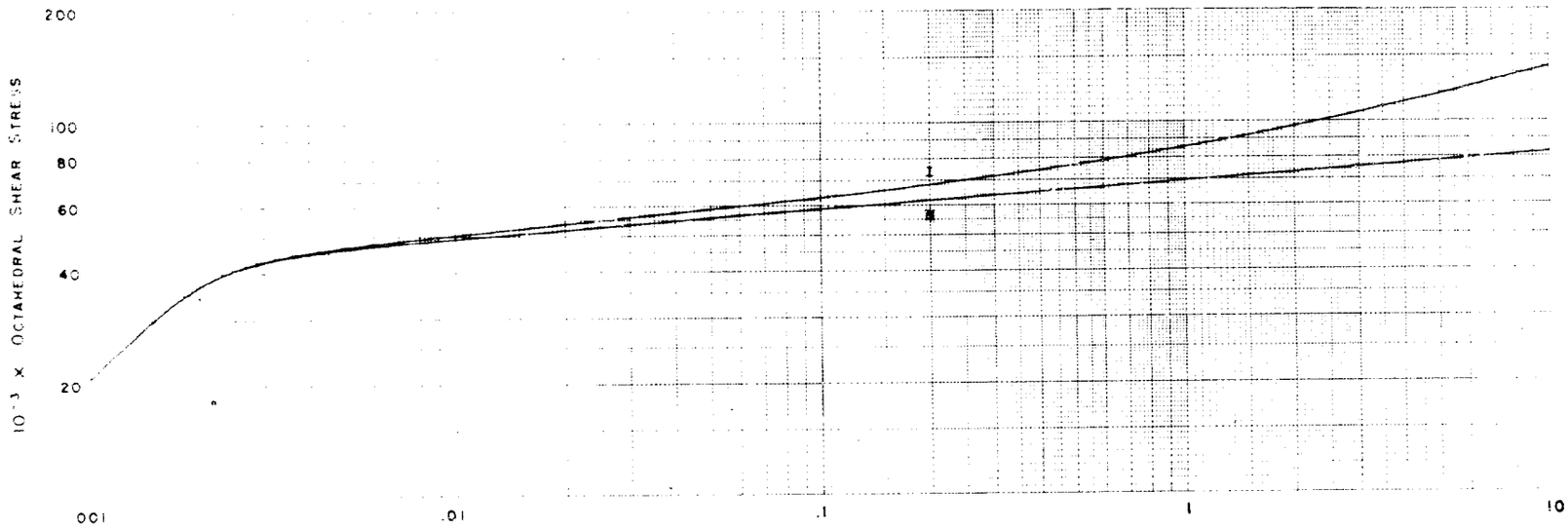

OCTAHEDRAL SHEAR STRAIN

CURVE I Tension or Compression

CURVE II Shear

NPG PHOTO NO. 3094 (APL) FIGURE (6)

STRESS-STRAIN CURVES

The Octahedral Shear Stress and The Temperature for an Adiabatic Deformation in Shear

STS of 115000 (lb)/(in)^2 Tensile Strength

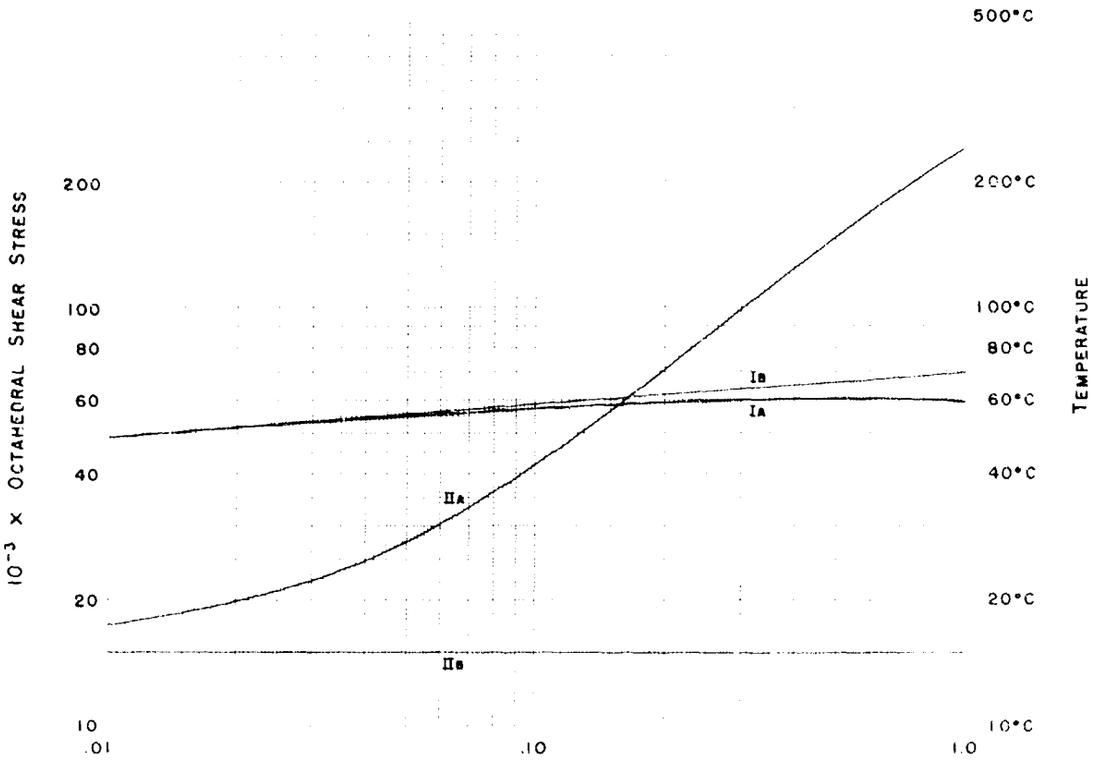

CURVE Ia Stress in an Adiabatic Deformation

CURVE Ib " " " Isothermal "

CURVE IIa Temperature in an Adiabatic Deformation

CURVE IIb " " " Isothermal "

THE VARIATION OF STRESS WITH TEMPERATURE

FIGURE (7)

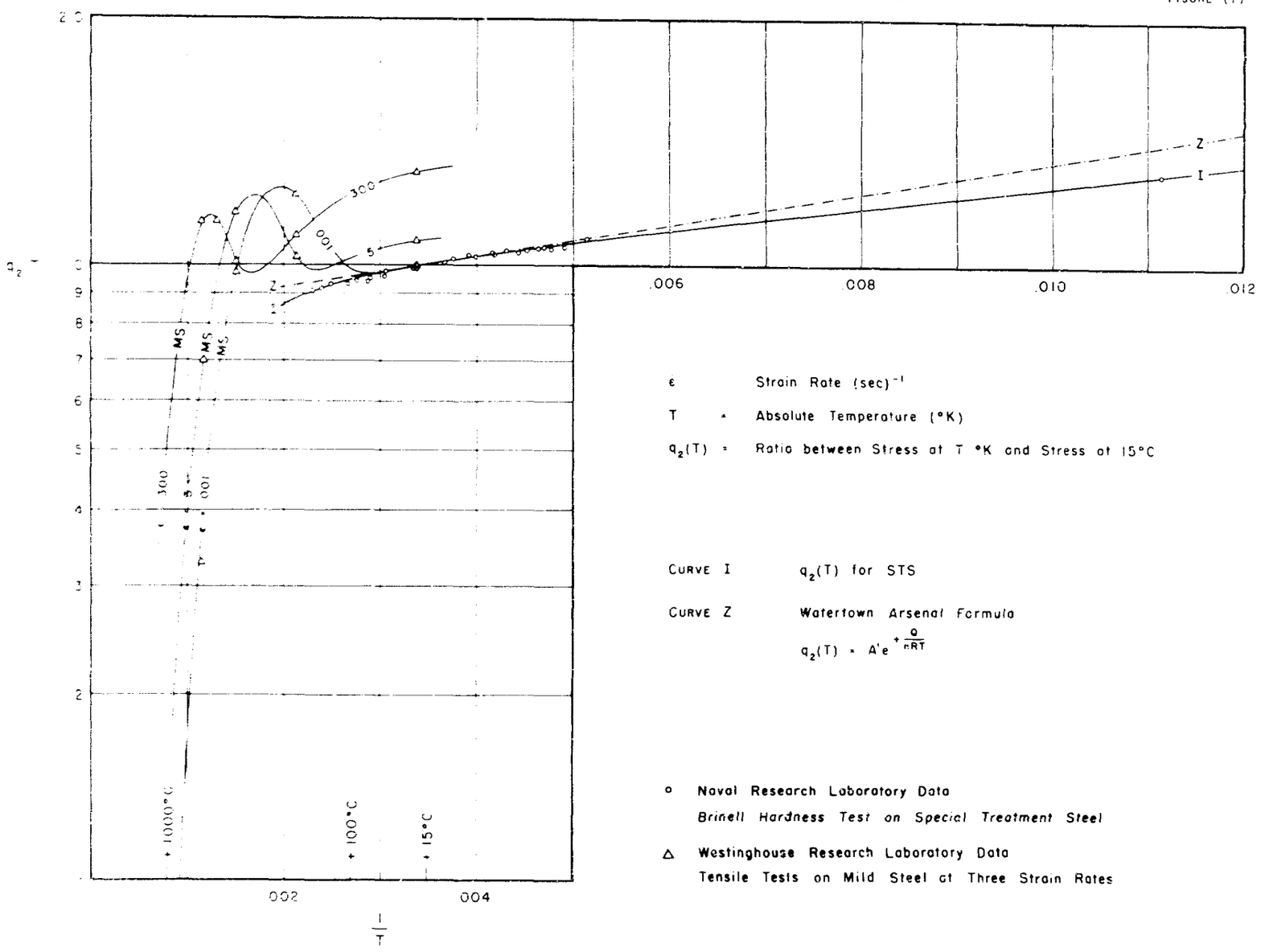

ϵ = Strain Rate $(sec)^{-1}$

T = Absolute Temperature (°K)

$q_2(T)$ = Ratio between Stress at T °K and Stress at 15°C

CURVE I $q_2(T)$ for STS

CURVE Z Watertown Arsenal Formula

$$q_2(T) = A'e^{+\frac{Q}{nRT}}$$

o Naval Research Laboratory Data
Brinell Hardness Test on Special Treatment Steel

△ Westinghouse Research Laboratory Data
Tensile Tests on Mild Steel at Three Strain Rates

THE VARIATION OF STRESS WITH STRAIN RATE AT 15°C

FIGURE (8.1

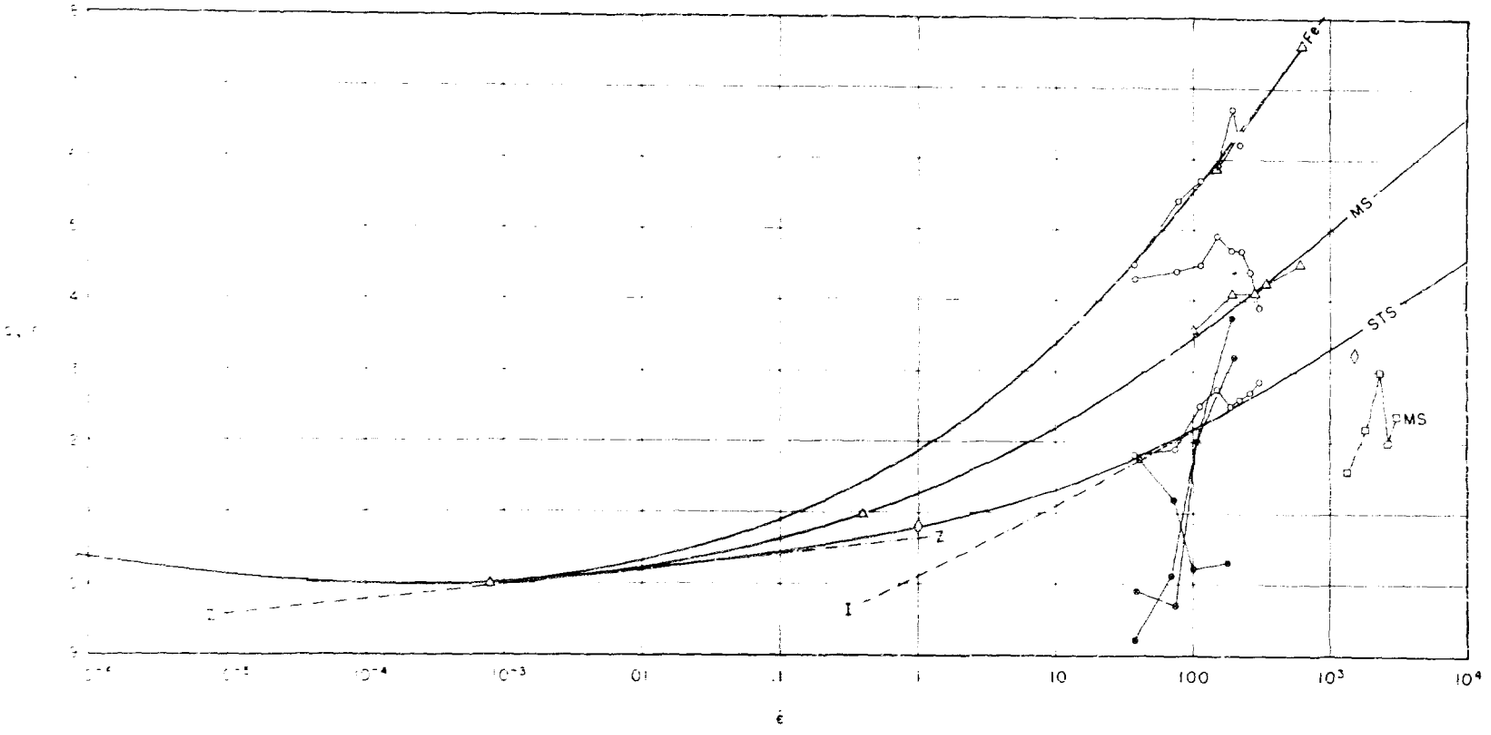

○ California Institute of Technology Data
Tensile Test Specimens in a Tensile Impact Machine

⊗ California Institute of Technology Data
Hollow Tubes under Internal Pressure

△ Westinghouse Research Laboratory Data
Tensile Test Specimens in a Rotary Impact Machine

▽ Carnegie Institute of Technology Data
Compression Test Specimens in a Rotary Impact Machine

□ Massachusetts Institute of Technology Data
Tensile Test Specimens in a Bomb with
Impact Velocity at von Karman Critical Velocity

$\dot{\epsilon}$ = Strain Rate $(sec)^{-1}$

$q_3(\dot{\epsilon})$ = Ratio between Dynamic Stress and Static Stress

Fe = Pure Iron

MS = Mild Steel

STS = Special Treatment Steel

CURVE I Naval Proving Ground Formula
$\log q_3 = + (.01) + (.04)\log \dot{\epsilon}$

CURVE Z Watertown Arsenal Formula
$\log q_3 = + (.06) + (.009)\log \dot{\epsilon}$

FIGURE (9)

THE DYNAMIC TENSILE STRENGTHS OF SEVERAL STEELS

Strain Rate = 200 $(sec)^{-1}$

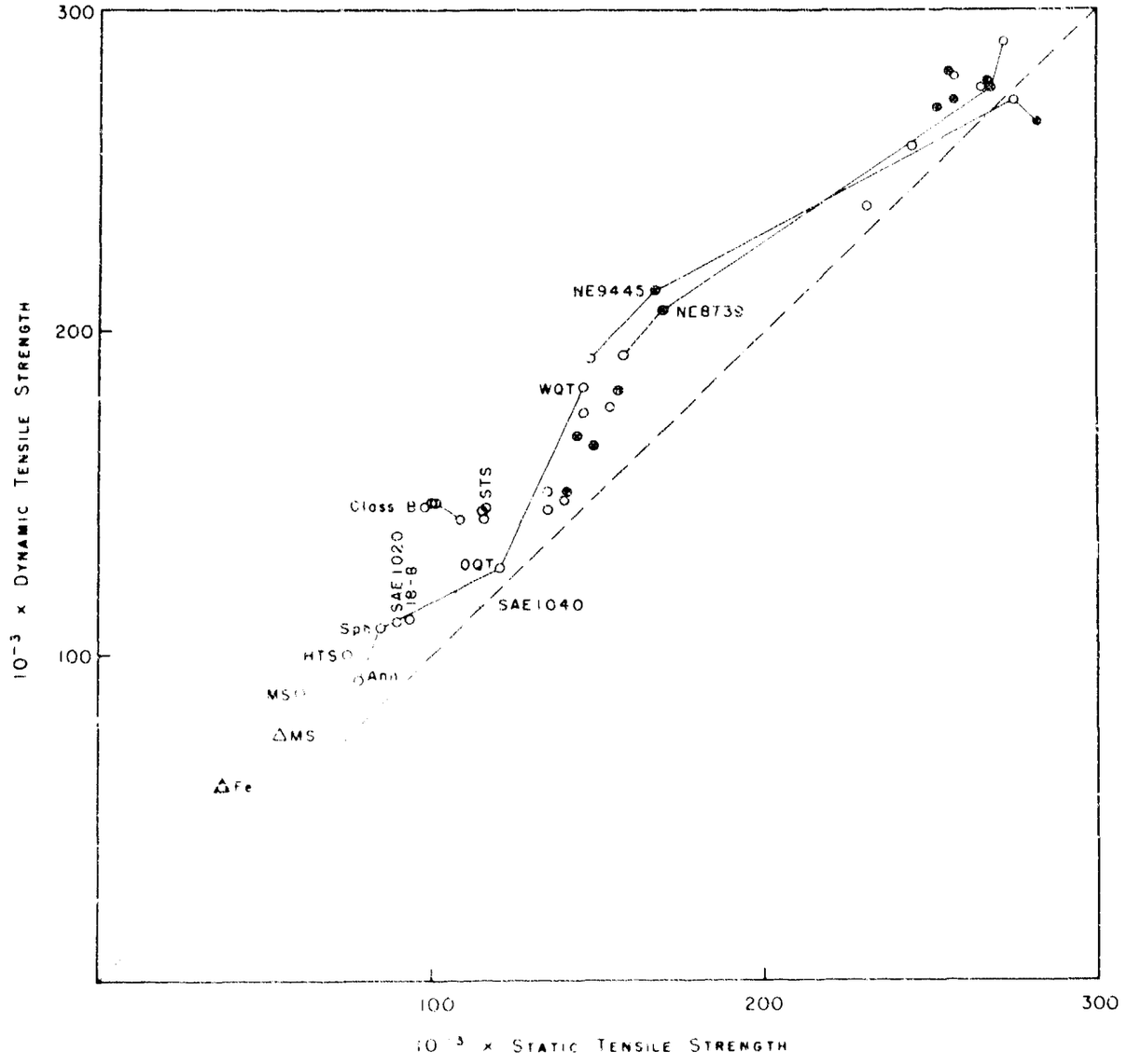

Fe - Pure Iron
MS - Mild Steel
HTS - High Tensile Steel
STS - Special Treatment Steel
Ann - Annealed
Spt - Spheroidized
OQT - Oil Quenched and Tempered
WQT - Water Quenched and Tempered

△ Westinghouse Research Laboratory Data

○ California Institute of Technology Data
Quenched and Tempered Steel

⊛ California Institute of Technology Data
Austempered Steel

NPG PHOTO NO. 3098 (APL)

FIGURE (10)

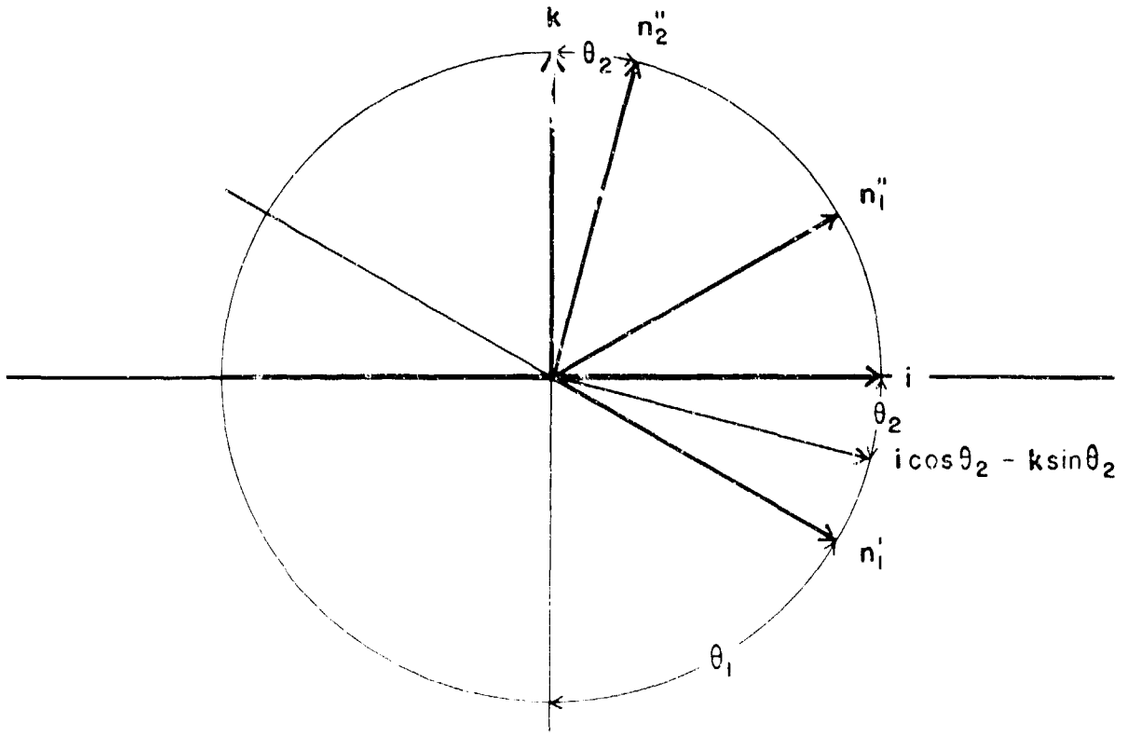

WAVE NORMALS AT A FREE BOUNDARY

NRG PHOTO NO. 3099 (APL)

FIGURE (11)

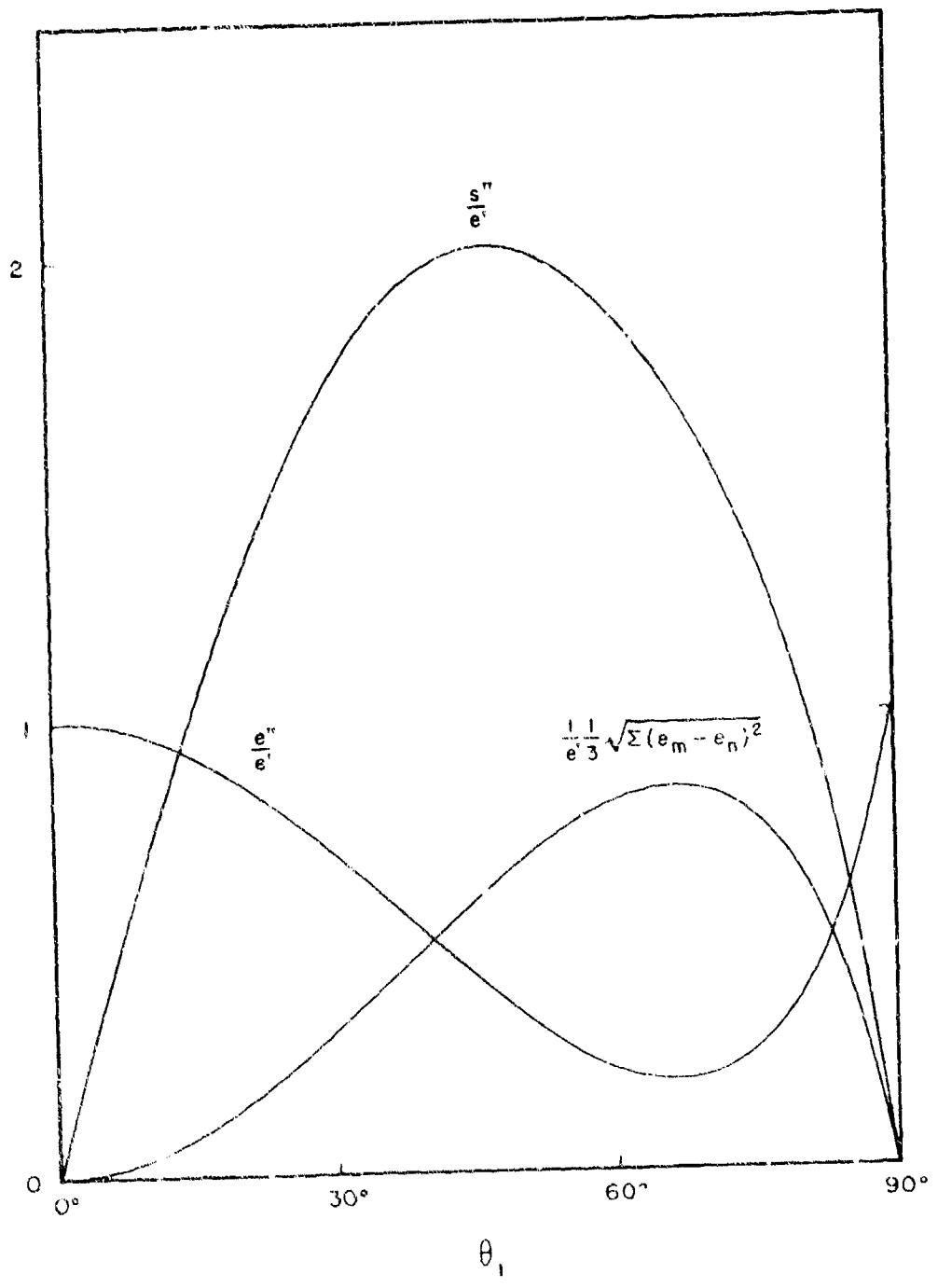

THE REFLECTION OF ELASTIC WAVES AT A FREE BOUNDARY

NPG PHOTO NO. 3100 (APL)

FIGURE (12)

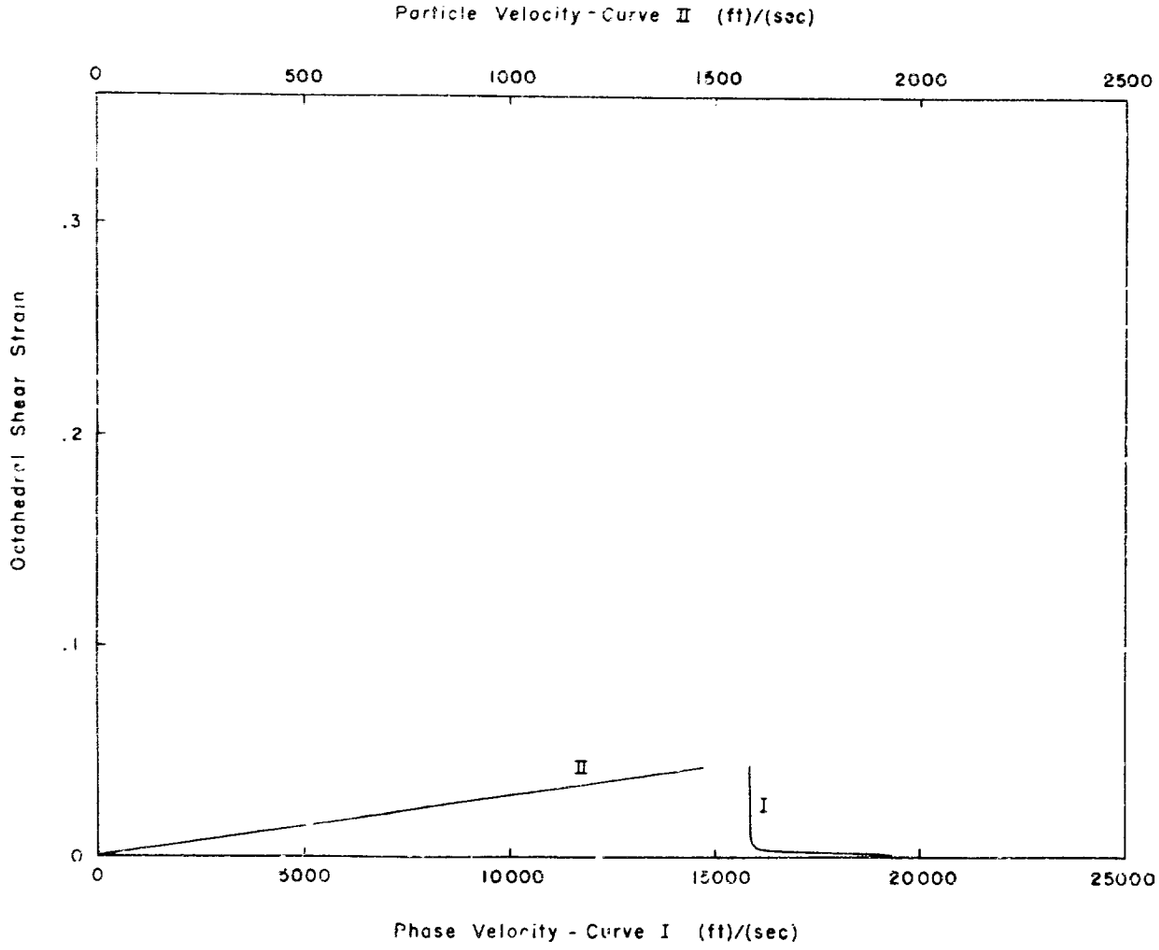

THE PROPAGATION OF LONGITUDINAL PLASTIC WAVES IN STS

NPS PHOTO NO. 3101 (APL)

FIGURE (13)

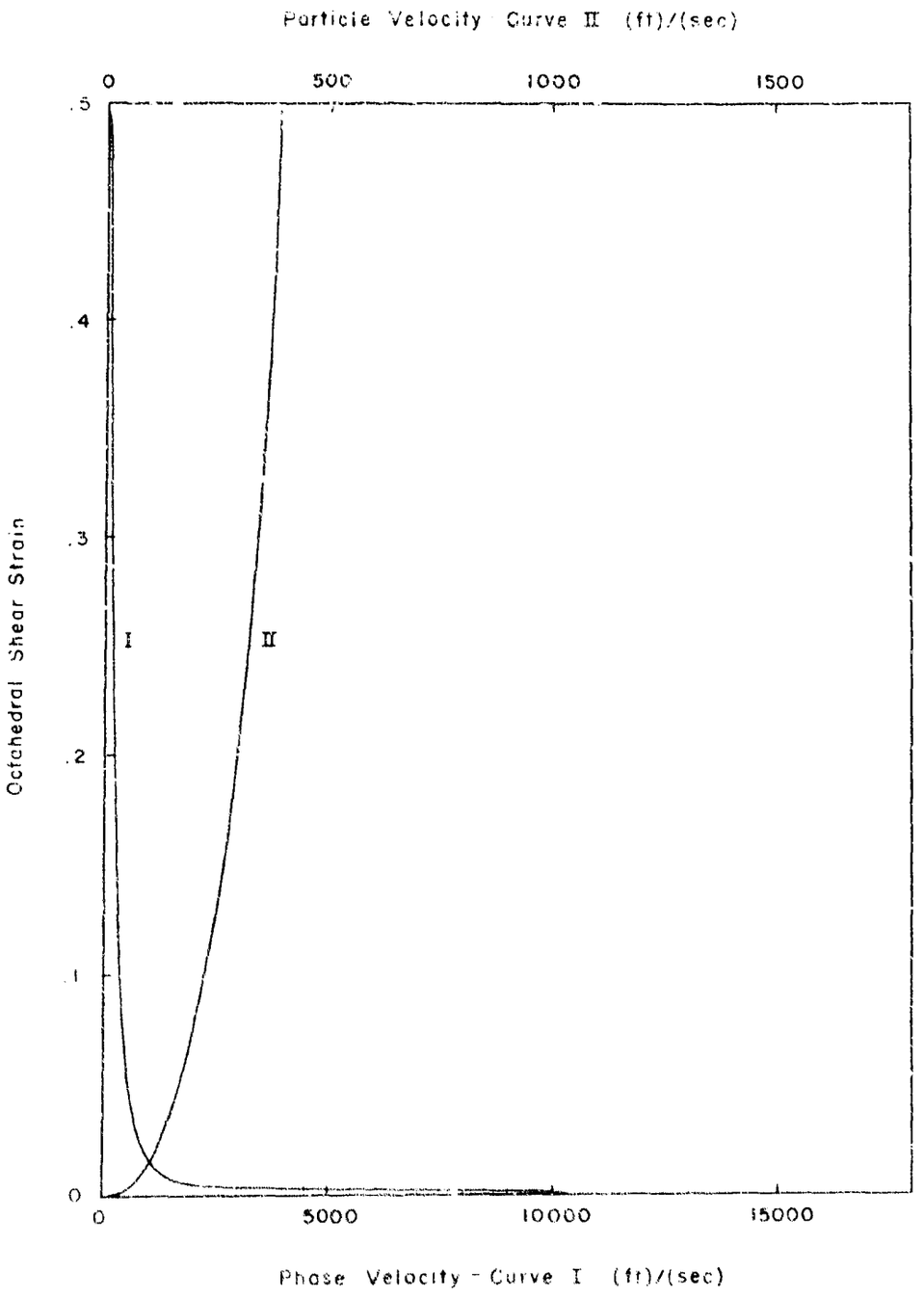

THE PROPAGATION OF TRANSVERSE PLASTIC WAVES IN STS

NPG PHOTO NO. 3102 (APL)

FIGURE (14)

THE MOMENT-CURVATURE RELATIONSHIP

STS of 115000 (lb)/(in)^2 Tensile Strength

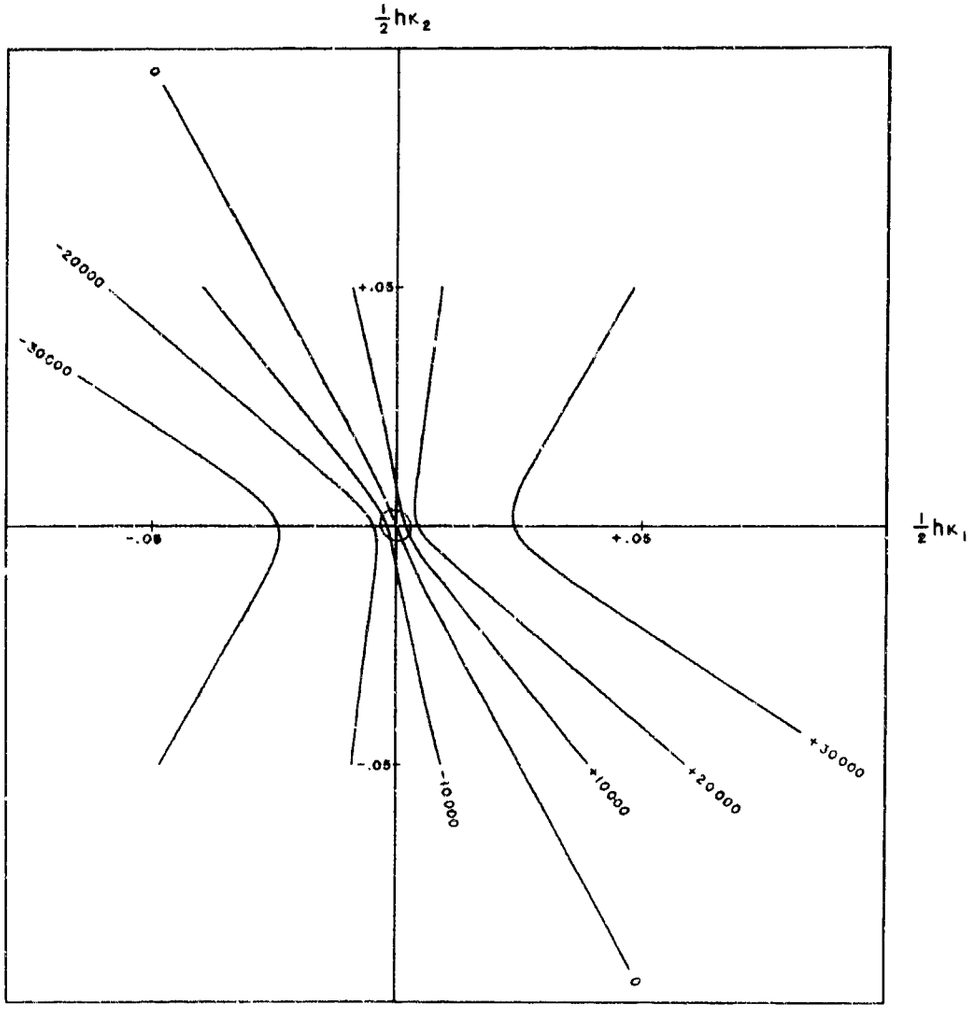

Contours of equal $\frac{1}{h^2}M_1$, expressed in (lb)/(in)^2

K_1, K_2 = curvatures of the plate

h = plate thickness

$\frac{1}{2}hK_1, \frac{1}{2}hK_2$ = components of strain at the surface of the plate

M_1, M_2 = force moments per unit length

The dotted ellipse marks the yield point